energies

MDPI

Review

A Comparative Review of Lead-Acid, Lithium-Ion and Ultra-Capacitor Technologies and Their Degradation Mechanisms

Ashleigh Townsend * and Rupert Gouws

School of Electrical, Electronic and Computer Engineering, North West University, Potchefstroom 2520, South Africa; rupert.gouws@nwu.ac.za
* Correspondence: ashleighktownsend2@gmail.com

Abstract: As renewable energy sources, such as solar systems, are becoming more popular, the focus is moving into more effective utilization of these energy sources and harvesting more energy for intermittency reduction in this renewable source. This is opening up a market for methods of energy storage and increasing interest in batteries, as they are, as it stands, the foremost energy storage device available to suit a wide range of requirements. This interest has brought to light the downfalls of batteries and resultantly made room for the investigation of ultra-capacitors as a solution to these downfalls. One of these downfalls is related to the decrease in capacity, and temperamentality thereof, of a battery when not used precisely as stated by the supplier. The usable capacity is reliant on the complete discharge/charge cycles the battery can undergo before a 20% degradation in its specified capacity is observed. This article aims to investigate what causes this degradation, what aggravates it and how the degradation affects the usage of the battery. This investigation will lead to the identification of a gap in which this degradation can be decreased, prolonging the usage and increasing the feasibility of the energy storage devices.

Keywords: lead acid battery; lithium-ion battery; ultra-capacitor; battery degradation; sulfation; stratification; renewable energy sources; energy storage; capacity decay/attenuation; charge/discharge cycles

Citation: Townsend, A.; Gouws, R. A Comparative Review of Lead-Acid, Lithium-Ion and Ultra-Capacitor Technologies and Their Degradation Mechanisms. *Energies* **2022**, *15*, 4930. https://doi.org/10.3390/en15134930

Academic Editors: Marcin Wołowicz, Krzysztof Badyda and Piotr Krawczyk

Received: 24 May 2022
Accepted: 23 June 2022
Published: 5 July 2022

1. Introduction

Energy storage is a key component required in the diversification of energy sources. Renewable energy source advances [1], as well as recent grid power regression [2], has highlighted the necessity of energy storage due to intermittency. Renewable energy is intermittent by nature, where the availability and extent of availability is limited by the source [3]. Intermittency refers to the discontinuous availability of electrical energy due to external factors that cannot be controlled and that occur in generating sources that vary over a short-time period [4].

Renewable sources that are intermittent include solar, wind, tidal and wave [5,6]; solar and tidal are relatively predictable due to weather, tidal and diurnal patterns [7]. The causes of intermittency in solar power are due to solar intensity variances throughout the day, and in different locations, as well as cloud cover [8,9]; wind power is considered highly intermittent as it has more variances with respect to wind speed, air density and turbine characteristics. These factors are further influenced by location [8,9]. Tidal (and wave) power is significantly more predictable as tides occur at expected times [7]. However, all of these generation sources are known as non-dispatchable sources as the output is not guaranteed at any moment to meet fluctuating energy demands [4].

Renewable energy is not only dependent on the availability; it is also dependant on the magnitude of the generative source of that energy [10]. If the source is insufficient (the system design is not large enough or has incorrect parameters, or the supply is intermittent [11]) no significant power will be generated, and if the load requirement is less than the source capacity, the remainder is lost [12]. By having a renewable source provide the

required load with any remainder supplying an energy storage device, i.e., hybrid energy storage systems (HESS), the renewable source can be utilized on a larger scale and more efficiently [13].

Currently there exists a multitude of energy storage technologies: pumped-hydro and compressed-air energy storage facilities, flywheels, superconducting magnetic storage and electrochemical energy storage [12]. The first four options are limited by their site-dependence [14–16], capacity [17,18] or response capabilities [15,19], whereas electrochemical energy storage (such as batteries and supercapacitors) offers more flexibility in capacity [20], siting and rapid response capabilities [21] that meet a larger range of applications [22] as compared to the other types of energy storage. Due to their versatility, high energy density, efficiency and cost, batteries have seen great growth in their application in energy storage systems [23].

Because batteries have become a staple in energy storage systems, the market has been flooded with different battery chemistries. Nickel based, lead-acid (LA), lithium-ion (LI) and alkaline are a few of the more commonly known batteries currently on the market, each with their own set of properties, as can be seen in the table of comparison (Table 1) from A. Townsend et al. [24]. Table 1 represents a comparison of the mentioned battery chemistries with the addition of zinc-oxide (Zn-O_2), sodium-sulphur (NaS) and vanadium flow (VFB) batteries as well as fuel cells (FC)—all of these will be discussed later in this article.

Table 1. Comparison of battery technology properties, adapted from [24–29].

		Battery Technology								
		LA	**NiMH**	**LI**	**NiCd**	**LiPo**	**Zn-O_2**	**NaS**	**VFB**	**FC**
Nominal cell voltage	V	2.1	1.2	3.6–3.85	1.2	2.7–3	1.45–1.65	1.78–2.208	1.15–1.55	0.6–0.7
Energy density	Wh/kg	30–40	60–120	100–265	40–60	100–265	442	240	25	1500
Power density	W/kg	180	250–1000	250–340	150	245–430	100	230	100	400
Cycle life	Cycles	<1000	180–2000	400–1200	2000	500	100	4500	>10,000	~9000 *
Charge/discharge efficiency	%	50–95	66–92	80–90	70–90	90	60–70	87	70–80	40–60
Self-discharge rate	%	3–20	13.9–70.6	0.35–2.5	10	0.3	0.17	2	~0	0
DoD	%	50	100	80	60–80	80	60–65	100	100	100
Cost	USD/Wh	0.69750	0.8546	0.9361	2.6778	2.3095	0.3095	0.5	5.7	0.02
TRL		9	9	9	9	9	9	7	9	9

* FCs are not measured with cycles; thus, this is approximated according to cycles per year of a battery where FCs have a lifespan of 12 years.

From Table 1, it can be seen that a few key properties are focused on when looking at batteries (a few of which can also be applied to FCs), the energy- and power-capacity (including current capacity and peak capability), depth of discharge (DoD), cycle life, cost, nominal cell voltage, availability, etc. [24]. It is often overlooked how each of these properties can affect one another; Figure 1 is used to illustrate this interdependence.

Referring to Figure 1, it can be seen that each characteristic is affected by the others [30]. All of these properties determine the capacity of the battery and there are many factors that contribute to, as well as ramifications that arise from, a reduction in the capacity [31]. The number of cycles is often used to determine the remaining capacity and, thus, the degradation of the battery [32,33]; this is shown in Figure 3 by P. Zhang et al. [8] and in Figure 11 by V. Sedlakova et al. [34].

This article aims to research this degradation (what leads to and arises from it) to determine how this degradation further impacts the continued use of the battery as well as to look into methods used to reduce this degradation.

2. Overview of Energy Storage Devices

As mentioned above, there are many different types of energy storage technologies, of which this article will focus on electrochemical devices, as these have a larger variation of applications. The energy storage devices (ESDs) that will be focused on in this section are LA/LI batteries and ultra-capacitors (UC). The exclusion of the remaining ESDs will be elaborated on in the subsequent section below.

2.1. Battery Technology

Batteries generally have a high energy-density-to-power-density ratio—this allows them to provide power for longer durations, but they generally do not efficiently supply peak power demands; they respond slowly to dynamic loads and they have low charge rates [35,36]. The various chemical compositions of each technology determine the characteristics of each battery. LI has lithium cobalt oxide (LCO), lithium iron phosphate (LFP), lithium manganese oxide (LMO), lithium nickel manganese cobalt oxide (NMC), lithium polymer (LiPo) and lithium titanate (LTO) [37]; LA has flooded, deep cycle, absorbent glass mat (AGM) and gel [38]; nickel based has nickel metal hydride (NiMH) and nickel cadmium (NiCd) [39]; alkaline has rechargeable and non-rechargeable [40]—these are the more commonly known variations. Zinc-oxide (Zn-O_2/Zn-air) [41], sodium sulphur (NaS/salt) [42] and redox flow batteries (RFB) [29] form part of the lesser-known battery technology category. Table 1 compares the majority of these battery technologies and is used to create the bar graph shown in Figure 2 This figure compares each individual value from the table with the highest value in that category to provide a clear indication of the frontrunners.

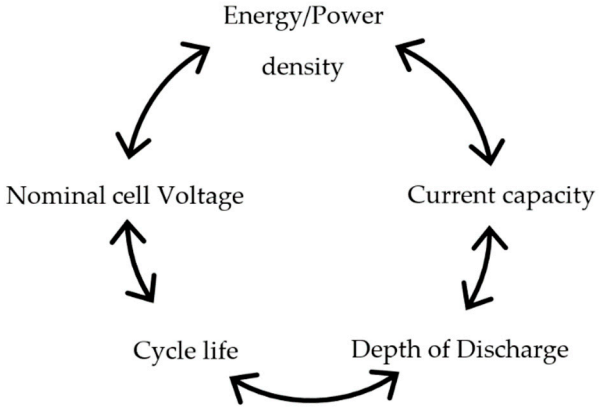

Figure 1. Battery key property interdependence, adapted from [30].

LA batteries are the oldest technology and are the first type of rechargeable battery ever made [43]. Therefore, their parameters have been used as the comparison baseline for the other technologies. They have a relatively low energy density, a short cycle life and a comparatively high self-discharge rate; however, they are of the cheapest technologies [44].

LI has the benefit of a higher energy density and longer cycle life than LA; however, it is more expensive [45,46]. The last statement gives insight into the continually large presence of LA batteries in the renewable energy-storage field, further substantiated by [47], which shows that cost reduction and cycle life are inversely proportional.

NiCd and NiMH batteries are most frequently used in portable electronic applications due to their low internal resistance, thus having the capability of either supplying high peak power surges (NiCd) or having high drainage capabilities (NiMH) [48]. Both of these battery technologies have a significantly higher cycle life than LA [39]. NiMH is the replacement for NiCd, as NiCd releases toxins such as lead, mercury and cadmium. NiMH has a higher energy density than NiCd but with a lower cycle life. However, NiMH is significantly more expensive than NiCd [49].

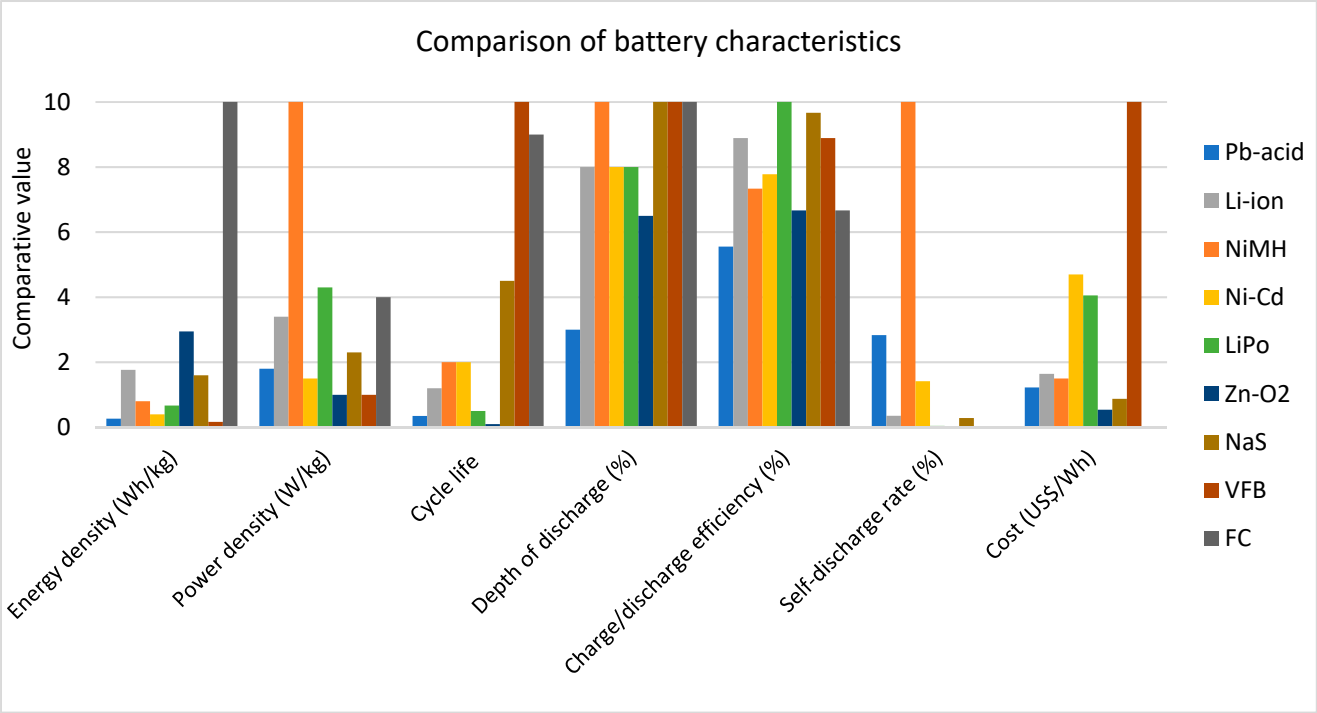

Figure 2. Comparison of different battery characteristics, adapted from [24–29].

Rechargeable alkaline batteries (such as Zn-MnO_2) have a very high internal resistance and similar power- and energy densities—both of which are higher than the LA technology [50]. This makes them suited for low-drain applications that have repetitive, but not continuous, use, i.e., periodical/intermittent use items [51]. Although these are the rechargeable version of alkaline batteries, their cycle life is significantly low—as low as 50 cycles, when used optimally [52].

Zn-O_2 batteries offer great advantages in energy density (the highest of all the mentioned types) with the future promise of high cycle life; they will be suited for long-use-low-power applications [53]. However, the technology does not currently permit such high recharge cycles [54]; thus, it is currently not an option.

NaS batteries offer great potential for renewable energy storage as they have 100% DoD with significantly high charge cycles, they have comparatively good energy- and power density and they have one of the lowest costs of all the mentioned technologies [55]. The one major downside of these batteries is the high operating temperature, limiting their applications [23,56]. Another factor to consider is that these batteries have a TRL of 7 and are thus commercially unavailable.

In a traditional battery, the electrons travel through the electrolyte between the electrodes; in an RFB the electrodes are the electrolytes [57]. RFBs are generally divided into two categories—true or hybrid [58]; the main difference is that hybrid RFBs have one oxidation state of the redox couples stored on the electrode surface as a solid [59]. Vanadium-vanadium and iron-chromium are examples of true RFBs and zinc-bromine and zinc-chlorine are examples of hybrid RFBs [27]. What makes these batteries so attractive is that they do not degrade as an LI battery would. Thus, they have a significantly longer lifespan [57], and they are easily scalable—the size of the tanks just has to be increased (volume of electrolyte used) [60]. They are considered safer than LI as the electrolyte is not flammable, and consequently they do not experience thermal runaway; they also have a very low, almost zero, self-discharge due to the active materials being separated when they are not being used [27]. On the downside, these batteries are not suited for portable applications [57], they have lower energy capacity and they are significantly more expensive due to the initial infrastructure setup requirements [57,61,62].

An alternative to battery technology is seen in the form of FCs [63]. There are various types of FCs—polymer electrolyte membrane (PEMFC), alkaline (AFC), phosphoric acid (PAFC), molten carbonate (MCFC) and solid oxide (SOFC) [64]. Each of these FCs have various differences: PEMFC and SOFC utilize a solid electrolyte whilst the others use a liquid variation (solid electrolytes have the advantage of less corrosion [65]). In order of being mentioned, operating temperatures and stack sizes increase, whereas susceptibility to carbon monoxide or dioxide poisoning decreases [64]. MCFC and SOFC have operating temperatures of 600–700 °C and 500–1000 °C [64], respectively, compared to a less than 200 °C operating temperature of the remaining variations [66]. Increased operating temperatures increase the start-up time and corrosiveness of the components but decrease the necessity for external fuel reformation or electrolysis. PEMFC and PAFC require a precious-metal catalyst which increases the cost significantly [64]. Susceptibility to poisoning [67], catalyst type [68], external fuel reformation or electrolysis requirements and higher operating temperatures all lead to an increase in the overall cost of the FC (higher operating temperatures increase corrosiveness and degradation of the components) [67].

FCs have the advantage of high energy density (similar to that of LI batteries), can be carbon-neutral (by-product of cell is water and heat [64]) [69], its capacity does not deplete during "discharge" (it supplies a constant capacity throughout) and "recharging" is as quick as a refuel (around 3 min) [70]. Most FCs use some or other form of hydrogen as fuel as hydrogen is abundant, but its acquisition requires either electrolysis or reformation [63]—herein lies the method of storing renewable energy, i.e., generate and store hydrogen. Hydrogen can be stored and transported in either liquid or gas form. The liquid form requires cryogenic temperatures and the gas form requires high compression rates [71]. Both have high energy losses (40% and 13%, respectively) which are large in comparison to those related to the transmission of electrical energy (±9%) [72,73]. Both methods of generation as well as the storage of hydrogen require significant infrastructure, which increases the initial investment for FC use [74]. Additionally, hydrogen can be highly flammable, which adds another investment level to the infrastructure requirement [75,76].

Summarizing the main disadvantages of the above technologies, in relation to renewable energy storage applications, NiCd and NiMH are generally made for applications requiring small current capacities; rechargeable alkaline and Zn-air have too few recharge cycles; NaS batteries can only be used in applications with low environmental temperature, but most importantly, they are not commercially available; and RFBs and FCs require too large of an initial capital investment and maintenance requirements. Initial cost, infrastructure and maintenance requirements, replacement frequency and operating temperatures give insight into why the above ESDs are not utilized more in the renewable energy storage industry, leaving LA and LI batteries. The acquisition and maintenance factors increase the complexity of ESD use [77]. LI and LA are most commonly used (and preferred) with renewable energy systems [78] (mainly due to their simplicity in terms of acquisition and maintenance) and will therefore be the focus of this article. Both LI and LA have multiple variations that differ in electrode chemistry, electrolyte viscosity and separator type. These variations will be discussed further.

2.1.1. Lead Acid Battery Technologies

LA batteries have sealed and flooded types—the former requires minimal maintenance, whereas the latter requires a larger amount of maintenance, more specifically in terms of electrolyte top-up [79]. However, for this article sealed LA batteries will be the focus as they offer better characteristics on all fronts except cost—the cost of a flooded LA battery is understandably lower than sealed as it requires maintenance by the user [79].

Deep-cycle LA batteries have thicker plates (than non-deep cycle types). This increases the density of the active material, increasing the energy density. More active material means deeper depth of discharge potential; however, this does not increase the cycle life [80].

Absorbent glass mat (AGM) LA batteries have a separator that is made of glass fibre [81]. This mat is only soaked in enough electrolyte to drench the mat. The mat allows

gasses from the chemical reaction to pass through and oxidize/reduce the opposing electrode. This gas would otherwise float to the top in the form of bubbles being released and lost into the atmosphere [49]. As this is a sealed battery [82], no top-up is required, allowing for minimal maintenance and a more robust design where leakage of the electrolyte does not occur, and the battery can be stored and used in any orientation [83]. This battery is often referred to as a valve-regulated-lead-acid (VRLA) due to the use of a blow-off valve intended to prevent over-pressurization of the battery from rapid/deep dis-/recharge [84].

Another advantage of AGM batteries is that the mat allows for significant compression, increasing energy density as compared to similar gel and liquid variations [85]. The mat also prevents vertical movement of the electrolyte; when the flooded variation is stored discharged, the acid molecules will gather at the bottom of the battery and when used, the current will then predominantly flow in this region, increasing the rate of deterioration of the plates [86].

The electrolyte can be replaced with a gel variation, formed through the addition of silica [87]. This delivers similar benefits to that of the AGM battery, except that the gel prevents rapid motion of the ions between the electrodes, thus reducing the surge current capability of the battery [88]. The above LA technologies are compared in Table 2 below.

Table 2. Lead acid battery technology comparison, adapted from [87,89–92].

	Energy Density (Wh/kg)	Power Density (W/kg)	Cycles	Cost * (USD/kWh)	Cost per Cycle (USD/kWh/Cycle)
Flooded	34.29	68.57	350	55.56	0.16
Deep cycle	40	52.80	500	186.72	0.37
AGM	41.38	153.97	600	142.86	0.24
Gel	35.82	125.37	750	168.06	0.22

* Based on R0.062/USD, 5 May 2022. All values are based on 12 V 200 Ah batteries.

When comparing LA battery technologies, the most important characteristics used are those listed in Table 2: energy density, power density, cycles and cost. The final column, cost per cycle, is predominantly used to obtain a better indication of the feasibility of the technology over the entire term of its documented cycle life. From Table 2, deep cycle batteries show an advantage over flooded batteries with respect to the energy density and cycles; however, both AGM and gel batteries show a significant improvement in power density and cycle durability. Flooded batteries have a significantly lower cost—more than 30% less—than the other technologies, which, despite their lower energy density and cyclability, further justifies their continued large presence in the market.

2.1.2. Lithium-Ion Battery Technologies

LI batteries operate through the intercalation and deintercalation of LIs into the electrodes' chemical structures [93]. Often a lithium salt is added to the electrolyte to reduce the travelling distance of the LIs, which facilitates faster reactions between the anode and cathode [94]. The LI battery is discharged once the cathode is fully intercalated with lithium [93].

A LCO cathode is the most common (and first) type of LI battery [95,96]. Due to its layered trigonal crystalline structure, cobalt oxide offers the highest energy density of all the LI variations but possesses a high thermal instability [97]. The anode can overheat, leading to the cathode releasing oxygen, and the electrolyte is usually also highly flammable, which exacerbates this fire hazard [98].

LFP, LMO and NMC offer three alternative cathode variations for LI batteries. The orthorhombic crystalline structure of LFP offers better thermal stability (due to iron-phosphate's high temperature tolerance), a longer cycle life and higher power density but also lower energy density and higher self-discharge than the cobalt variation [99]. The cubic crystalline structure of LMO offers very good thermal stability [100], lower internal

resistance and thus high power density (although lower than the other variations), but it has a lower capacity and cycle life [101]. Finally, NMC (with a trigonal crystalline structure) combines the LCO and LMO technologies to obtain a high energy density (still lower than the cobalt variation), with low internal resistance and thus high power density and good thermal stability (from LCO) [102].

The liquid electrolyte can be replaced with a thin solid polymer to introduce another LI variation—LiPo [103]. With a solid electrolyte, the once rigid construction is now flexible, more compact, lighter and safer, allowing for a higher energy- and power density. However, the polymer tends to be very insulative; thus, a small quantity of gel is added to improve the conductivity [103,104].

LTO is a variation of the anode that contains a layered monoclinic/olivine crystalline structure, where the cathode of this variation is manganese oxide or NMC. This construction allows for high cycle life and power density but a very low energy density [105]. This battery has no solid electrolyte interface (SEI) film formation and thus no morphological degradation; it has a deeper and faster discharge (and charge) than the other variations and no lithium plating occurrence. Furthermore, it is thermally stable and has better low temperature functionality than the other battery types [106]. These various technologies are compared using Table 3 below.

Table 3. Comparison of lithium-ion battery technologies, adapted from [95–102,105–112].

	Energy Density (Wh/kg)	Power Density (W/kg)	Safety/Thermal Runaway (°C)	Maximum Discharge/ Charge C-Rate	Cycles	Cost * (USD/kWh)	Cost per Cycle
LCO	150–200	50–100	150	1/1	500–1000	385	0.39–0.77
LMO	100–150	250–400	250	10/1	300–700	400	0.57–1.33
NMC	150–220	100–150	210	2/1	1000–2000	420	0.21–0.42
LFP	90–160	200–1200	270	25/2	>2000	580	0.29
LTO	50–80	3000–5100	280	10/10	>5000	1005	0.14–0.34

* The cost values presented are based on the values obtained around 5 May 2022 and R0.062/USD. These values are for Li-ion cells with a nominal cell voltage between 3.2 and 3.6 V for consistency.

When comparing LI battery technology, the most important characteristics used are those listed in Table 3: energy density, power density, thermal runaway, maximum charge- and discharge rates, cycle durability and cost. The cost per cycle is predominantly used to determine the feasibility of the specified technology. From Table 3, LTO has very desirable characteristics—it has the highest thermal stability and lowest cost per cycle. Its high-power density, coupled with the high c-rate, allows for fast charge and discharge; however, the low energy density limits its application to those requiring more immediate power and not prolonged power. NMC comes in second with respect to cost per cycle; it has the best energy density (along with LCO), good thermal stability and cycle durability; it is, however, limited by its c-rate and power density to applications with lower peak power requirements. LFP presents a good all-rounder, with low cost per cycle, high cycle durability, great thermal stability and discharge rate and comparatively good energy- and power density. LMO offers an improvement on LCO in terms of energy density, thermal stability and discharge rate. However, LCO has better cyclability, thus lowering the cost per cycle significantly.

It is important to note that the thermal runaway temperature is a very important factor to consider for the application of LI technology, as the battery is sealed, and the electrolyte can be very volatile in terms of flammability and explosivity [97,113,114].

2.2. Ultra-Capacitor Technology

An ultra-capacitor is a capacitor that has an ultra-high capacitance but with a lower voltage limit [28]. It is an ESD that essentially combines electrolytic capacitors and rechargeable batteries—storing 10–100 times more energy per unit volume than the former and

being capable of accepting/delivering charge much faster and tolerating significantly more re-/discharge cycles than the latter [115].

Different from ordinary capacitors, UC do not use a conventional solid dielectric—they make use of an electrolyte and isolative membrane and they replace the material of the plates with one that is (more) porous. The latter allows for a larger effective surface area, whereas the former allows for the formation of an electric double layer- (EDL) and electrochemical pseudo (EP) capacitance, which together form the total capacitance [116]. When the EDL-capacitance exceeds the EP- capacitance, the UC is referred to as an EDL capacitor; otherwise, it is an EP capacitor [117]. There are mainly three types of UC: EDL-, EP- and hybrid capacitors (HC) [118].

In EDL capacitors, the energy storage and release is based on nanoscale charge separation at the interface formed between the electrode and electrolyte [26,119]. The charge storage mechanism is electrostatic (a physical charge transfer), allowing EDL capacitors to have relatively long life cycles [26,120,121]. EP capacitors store charge on the basis of faradaic redox reactions (electrochemical storage) involving high energy electrode materials. These electrode materials allow supercapacitors with higher energy density at the price of shorter life cycles and lower charge/discharge rates than EDL capacitors [120,122–126]. HCs are the hybrid combination of mechanisms from both EDL- and EP capacitors [118].

UC generally have a higher power-density to energy-density ratio, allowing them to provide bursts of high power for short durations. Their internal resistance is very low, thus allowing for little restriction when providing or receiving power [127]. Opposite to batteries, UC function best in intermittent high-power applications and do not fare well with continued average-power requirements. They have an almost infinite cycle life and they have a low self-discharge rate, but they are relatively expensive as compared to battery technology [128].

EDL capacitors have highly porous and conductive electrodes, thus having the benefit of larger cyclic ability and little degradation due to the highly reversible non-faradaic reactions. Their main limitation lies in the requirement of these highly conductive electrodes, limiting EDL capacitors to carbonaceous materials. EP capacitors have higher energy densities, but lower cyclic ability and power density, than their EDL counterparts, due to the faradaic redox reactions. HCs consist of both polarized (carbon) and non-polarized (metal or conducting polymer) electrodes in order to obtain the high energy density and power density observed by EDL and EP capacitors. This allows for better cyclic ability at lower costs [129,130]. The three different types of UC are compared using Table 4.

Table 4. Comparison of ultra-capacitor technology, adapted from [131–134].

	Energy Density (Wh/kg)	Power Density (W/kg)	Cycle Durability	Operating Temperature (°C)	Cost * (USD/Wh)	Cost per Cycle	TRL
EDL	0.9–2.5	900–10,000	>1000 k	−40–+70	219.80	0.00022	9
EP	1–10	500–7000	>100 k	−20–+70	N/A **	N/A **	4
HC	5–55	250–5000	>20 k	−20–+70	103.90	0.00519	9

* Based on R0.062/USD, 5 May 2022. ** EP capacitors are only at laboratory environment test phase (TRL 4)—not available for commercial use or purchase

When comparing UC technologies, the most important characteristics are as listed in Table 4: energy density, power density, cycle durability, operating temperature and cost. The cost per cycle is predominantly used to determine the feasibility of the addition of UC to a system. As UC are generally used for their power density, the energy density is not as much of a concern as it is for the battery technologies.

Table 4 confirms what has been said above: EP capacitors have higher energy density but lower power density than EDL capacitors. It is also seen that HCs show a lower power density and cyclic ability than the other two but a higher energy density. Finally, it is observed that the EDL technology is significantly cheaper than the HC technology per

cycle, which can be attributed to the low cycling ability of the HC. The ESD technologies discussed above can be compared using a summary table, Table 5 below.

Table 5. Lead acid, lithium-ion and ultra-capacitor comparison, adapted from [24].

	LA	LI	UC
Energy density (Wh/kg)	35–40	50–220	2.5–55
Power density (W/kg)	69–154	50–5100	5000–10,000
Cycle life	800	3000	>50,000
Self-discharge rate (%pm)	<3	<2	>54 *
Operating temperature (°C)	−40–+60	−50–+85	−40–+70
Cost (USD **/kWh)	55–168	385–1005	103 k–220 k
Cost per cycle	0.07–0.32	0.14–1.13	0.22–5.19

* 1.8% per day according to [135]. ** Based on R0.062/USD, 5 May 2022.

It is clear, from Table 5, that the LI technology trumps LA in most categories, except cost. However, in relation to the quantity of cycles and the type of LA or LI technology, the cost of LI can be less than that of LA over its usable lifetime. UC, on the other hand, exhibit opposing behaviour with respect to energy- and power density and a significantly higher initial procurement cost and cost per cycle. Using these values from Table 5, Figure 3 is obtained, which compares the characteristics of the ESDs as ratios of each other.

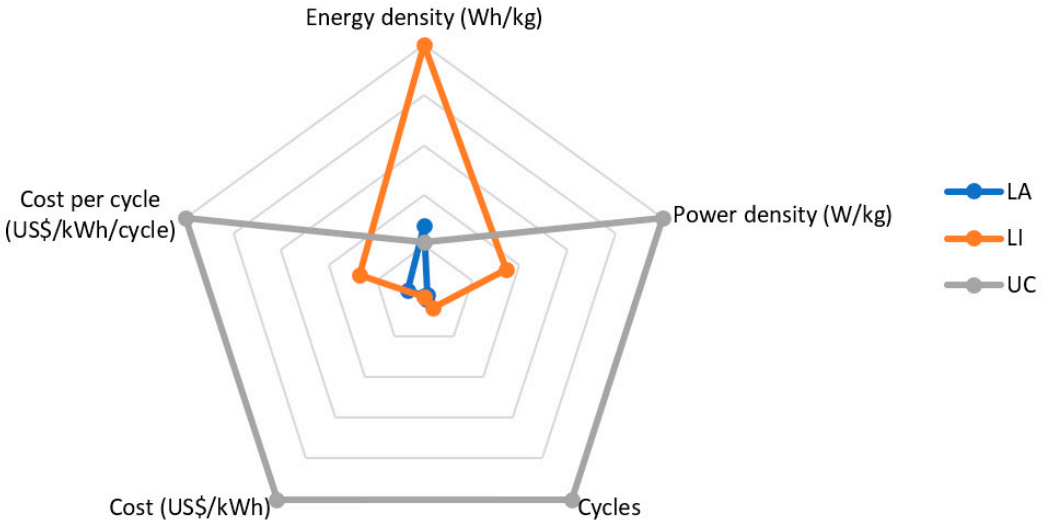

Figure 3. Radar graph comparing lithium-ion and lead acid characteristics, adapted from [24].

From this graph, it is clear as to why the UC is of interest as it exhibits opposite values of the energy-to-power-density ratio as compared to both the LI and LA technologies. The LI battery also shows better characteristics as compared to the LA, except when referring to cost, where it is slightly more expensive.

2.3. Separator Technology

The operation of the above mentioned ESD technologies depends on the properties of their main components—the electrodes, electrolyte and separator [136,137]. There are a few properties that are focused on when choosing a separator; the selection of these properties can affect both the degradation of the separator as well as of the ESD [138]. This degradation will be discussed under the appropriate section later in this article. The properties that are focussed on when choosing a selector are, amongst others, pore size, porosity, permeability, electrolyte wettability, mechanical properties, chemical stability,

ionic conductivity, ion migration and storage, thickness, dimensional stability, thermal stability and shrinkage, shutdown effect and cost [139].

Pore size (ideally <1 µm [140]) determines electrolyte storage, which ensures smooth ion transfer between the electrodes [109]. Larger pores improve transfer of ions, which increases the charge/discharge rate of the ESD. If they are too large, this allows transfer of cathode active material particles, which can lead to a short circuit between the anode and cathode [141].

Porosity determines electrolyte storage capacity and rate of ion conductivity of the separator [142]. Increased porosity leads to better ion conductivity (ideally 40–60% [139]) due to lower internal resistance and thus increased charge/discharge rate, more uniform distribution of the current and a lower chance of a short circuit. However, the higher the porosity, the lower the thermal and mechanical stability [143].

Thermal stability and -shrinkage refer to the functionality of the separator close to or at thermal runaway temperatures—it must not lead to or further aggravate thermal runaway [142]. Minimal shrinkage (<5% at 150 °C [140]) or piercing should occur at high temperatures [144].

Mechanical stability is related to tensile strength (robustness), elongation at break (tensile performance) and puncture strength (possibility of piercing through the material) [142]. High tensile and puncture strength is ideally desired (<2% [140]), as this leads to increased robustness and decreased possibility of piercing of the separator due to rough electrodes or growth formations (dendrite or crystal sulfation) on electrodes [145]. However, tensile strength is inversely proportional to porosity and ionic conductivity—thus, higher values increase internal resistance. Lower values will lead to the possibility of short circuiting between the electrodes, which can lead to or aggravate thermal runaway [139].

Ionic conductivity refers to the ability of ions to traverse through the separator between the electrodes [146]. Higher conductivity leads to lower internal resistance and better charge/discharge properties; however, this can also lead to the transfer of cathode active material particles to the anode, causing a short circuit and decreasing the service life of the battery [142].

Permeability is the ease of ion flow through the separator [142]. It is desired that the permeability be uniformly distributed throughout the separator. Low uniformity leads to higher internal resistance and uneven distribution of the current, which leads to higher chance of short circuits and thus decreased service life [145].

Electrolyte wettability refers to the hydrophilicity or hydrophobicity of the separator [142]. High wettability implies fast absorption, which leads to lower electrolyte loss, even distribution, sufficient storage, smoother ion transmission and lower internal resistance [147].

Chemical stability is the tendency of the separator to react with the electrolyte active materials. The separator reaction decreases the service life of the ESD and degrades the separator significantly [142].

Thickness of the separator affects the overall volume, energy density, specific capacity, cycle stability and safety of the ESD [142]. The ideal thickness is around 25 µm. An overly thick separator leads to increased contribution to the volume of the ESD, which reduces energy density and increases ion transmission distance, leading to slower charge/discharge rate. An overly thin separator decreases the mechanical strength and increases pierce-ability, and thus susceptibility to breakage, of the separator due to high currents [148].

Dimensional stability is related to the assembly process of the ESD [142]. When the battery is assembled, the electrolyte is dripped onto the separator—the absorption can cause shrinkage or curling which leads to wrinkles [149]. Wrinkles lead to uneven distribution of electrolyte and current which increases growth formations and decreases service life. Excessive shrinkage can lead to gaping at the edges, allowing the electrodes to electrically connect and short circuit [148].

The shutdown effect is the ability of the separator to melt and close pores at high temperatures to prevent further reactions between the electrodes that can lead to the dangerous operation of the battery [142]. Shutdown temperature must be lower than,

but close to, the thermal runaway temperature of the battery (±130 °C). If too low, the battery will malfunction too quickly, reducing service life; if too high, no benefits will be obtained [148].

The production cost of the separator is ±20% of the total battery cost and is related to the preparation of the separator [142]. Ideally, it is desired to keep this as low as possible, thus the existence of the various separator materials and continuous research and improvements in this field [149].

Ideally, the separator should meet all of the specifications [102]; however, the best value for all of the properties cannot be achieved at the same time, as many are inversely proportionate to each other [150]. Therefore, necessary performance parameters are augmented in lieu of the appropriate parameters for the specific application (some applications prefer higher charge/discharge rate, whereas others prefer robustness and thermal stability) [139,142].

LA batteries most commonly use AGM, polyolefin (PO) resin (from polyethylene—PE or polypropylene—PP), cellulose, etc. [151]. LI batteries generally use multi-layered separators to improve the individual characteristics of each, such as PO in multiple-layered-configurations (PE sandwiched between two layers of PP or a combination of single-layered PE and PP), a variant of these configurations which includes a ceramic-coated separator, ethylcellulose-modified PE between silicon-oxide (SiO_2)-nanoparticles-doped-polyimide, etc. [152,153]. Furthermore, UC use cellulose, polyethylene terephthalate (PET), PE, PP, polyvinylidene difluoride (PVDF), etc. [154].

AGM, reducing maintenance and leakage of the electrolyte [49,82,83], allows for significant compression, increasing energy density [85] and preventing vertical movement of the electrolyte for storage and usage in any orientation [83].

PO is derived from PP, PE or a lamination of the two [155,156]. They are the most commercially used separators due to the low production cost, higher mechanical strength and electrochemical stability [109], but they have low electrolyte absorption, are hydrophobic, have poor wettability, low porosity, poor thermal stability and a low thermal deformation temperature (80–85 °C and 100 °C, respectively), leading to thermal shrinkage and short circuits [157–159]—all of these decrease battery cycle life [139]. They are usually used in a PE/PP or PP/PE/PP configuration due to their individual characteristics; PE has good flexibility but a low melting point (130 °C), whereas PP has good mechanical properties and a high melting point (165 °C) [139,160]. The combination of the two therefore leads to low closed cell temperature and high fusing temperature, improved cyclability and safety performance of the battery [102].

Multi-layer variations improve stability and safety [161], and the addition of a ceramic-coated separator improves on the thermal stability [152]. The ethylcellulose variation is used in high performance batteries that accommodate both thermal runaway at high temperatures and thermal shutdown at low temperatures [139].

Cellulose, a constituent of plants and microorganisms [103,104] has better electrolyte uptake, interface stability and enhanced ionic conductivity [142,162], as compared to PP. It can improve the rate capability [163], cycling retention and thermal dimensional stability of the ESD [164]. Cellulose shows good flame retardancy, superior heat tolerance and proper mechanical strength [165].

PET has excellent mechanical, thermodynamic and electrical insulation properties, with the best form of this product being one with composite film with ceramic particles coated on the PET membrane. It shows excellent heat resistance with a high closed cell temperature of 220 °C [113].

Compared to PO, PVDF-based separators are characterized by strong polarity, high dielectric constant, stable electrochemical performance, excellent tensile properties and mechanical strength and favourable thermal stability and wettability [114–116]. They are also hydrophilic [166,167]. According to R. Liu et al. [114], PVDF has better porosity, electrolyte wettability, ionic conductivity and thermal stability as compared to PO, with similar chemical stability [107–112].

Separator engineering presents a formidable strategy in the improvement of battery and UC operation, specifically in suppressing growth formations [140]. Advances in separator technology have found that traditional PO separators are mechanically insufficient and thermally unstable, whilst multi-layer and ceramic coated self-shutdown separators show promise in their partial improvement of mechanical and thermal stability [152]. Tables 5 and 6 in B. Boateng et al. [140] present three techniques that show improvement of the downfalls of the current/most commonly used separator technologies and the performance that each obtains. Surface modification (employing various surface coating methods); single-layer (blending/doping of polymer substrates); and multi-layer (layering of substrates) are discussed, which all lead to improved performance and decreased growth formations. A. Heidari et al. [168] presents a discussion of surface modifications based on grafting methods, a mussel-inspired technique and functionalization by inorganic nanostructures that show promising improvements to the operation of ESDs. These methods also present a reduction in growth formations. J. Li et al. [169] presents the use of free-standing cellulose nanofiber to reduce polysulfide shuttle effect and dendrite growth, which results in an increase in discharge capacity. S. Thiangtham et al. [170] presents the use of bio-membranes based on a sulfonated cellulose blend that provides a variety of characteristic improvements, such as better ionic conductivity, higher discharge rate and better capacity retention whilst increasing porosity.

These mentioned case studies show that, although some of the separators have inferior performance characteristics, they can still have relevance through various construction techniques or combinations with other substrates. This alludes to the significance of the study into separator technologies and their degradation contribution with various ESD applications.

3. Degradation of Energy Storage Devices

Degradation is a big concern for long-term, reliable applications (electric vehicles, battery energy storage systems, aerospace systems) where long cycle life under continuous heavy loads is required. It is also important for managing its functional status to avoid operation under hazardous conditions [171]. There are a variety of factors that lead to degradation in the various types of ESDs, dependent on their technologies and chemical makeup. These various factors are discussed below, specifically regarding LI, LA and UC technologies. The causes, long term effects and possible reduction in the degradation will be discussed.

3.1. Lead Acid Battery Technology

LA batteries are often the first choice for photovoltaic systems due to their mature technology, making them a reliable choice, and their low cost makes the purchase more feasible. However, this technology is essentially the weakest of all the batteries, thus effectively making it the most expensive [172]. For this reason, research into the mechanisms that lead to degradation is of great concern. There are several mechanisms that can contribute simultaneously to the degradation; however, each individual battery has one dominant mechanism that determines its shelf life [173]. The major aging process in LA battery technology can be attributed to anodic corrosion, positive mass degradation, irreversible formation of lead sulphate in the active mass, short-circuits and loss of water. This all depends on the interrelationship between the charging/discharging regime, the DoD used throughout its life, prolonged periods of low discharge and average operating temperature [174].

The various types of LA batteries mentioned above have a capacity loss (cyclic and user-dependant) over time, which is summarized in Table 6 below.

Table 6. Causes of degradation in lead acid batteries, adapted from [87,174–180].

Type	Description	Consequence
Over-discharge	When the battery is discharged lower than the recommended DoD voltage. As the battery discharges lead sulfation accumulates on the surface of the electrodes; if over-discharged this sulfation crystalizes. Also leads to overexposure of the electrodes.	Crystal sulfation formation and electrode corrosion Effective surface area of the electrode is reduced, power density, overall capacity and cycle life of the battery is reduced. Extreme case—crystal sulfation will occupy the majority of the battery and the battery will be rendered useless; electrode corrosion will lead to collection of active material at the bottom of the battery which can potentially lead to a short circuit between the electrodes.
Over-charge	When the battery is left to charge for extended periods of time after reaching full charge status. For both FLA and SLA, heat leads to an increase in current transfer rate, which increases the chances of overcharging. The process of recharging this battery releases a lot of heat which is exacerbated when continued indefinitely.	Excessive heat— Leads to mechanical damage (warping of collector plates, shutdown of separator); evaporates the water in the electrolyte, increases acidity of the electrolyte and exposure of the electrodes; both increase the rate of corrosion, decrease the effective surface area, capacity, power density and service life of the battery. Extreme case—the evaporated hydrogen and oxygen cannot escape (larger risk in SLA) which poses a highly combustible and explosive hazard.
Crystal sulfation	When battery remains in extended state of discharge (partially/fully). Soft lead sulfation formed during discharge becomes hard crystals that cannot be broken down.	Effective surface area is reduced— Reduces power density, capacity and cycle life of the battery; Can also lead to damage of the separator (to be discussed under separator section of this article). Extreme case—crystal sulfation will occupy the majority of the battery and the battery will be rendered useless.
Stratification	Acid molecules in electrolyte gather towards the bottom of the battery. When a battery is stored discharged (partially/fully), the acid molecules separate from the water molecules.	Causes current flow predominantly in the acidic area increasing corrosion/wear of the electrodes.
Water loss	Any action that leads to loss of the liquid electrolyte or water element of the electrolyte. Mainly attributed to heat or leakage of the electrolyte. Heat is attributed to excessive environmental temperatures, high charge/discharge current or short circuits.	Decrease in volume of electrolyte— exposes the electrodes, increases electrolyte acidity and electrode corrosion, decreases effective surface area, power density and cycle life.
Short-circuit	When the electrodes are electrically connected and allow conduction between them. Caused by ineffective separator (poor battery assembly, defective, rough electrodes), collection of active material at the bottom of the battery (due to damage of the electrode from stratification or other causes), presence of conductive materials inside the battery (during assembly or maintenance of FLA batteries) or warping of the collector plates due to excessive heat.	Excessive heat generation— reduction in water concentration of the electrolyte, increase in acidity, increased corrosion of the electrode, decrease in overall battery capacity and subsequently, of the service life thereof.

3.2. Lithium-Ion Battery Technology

The capacity of a LI battery degrades due to a wide range of mechanisms, some that occur simultaneously and some that trigger further mechanisms [181]. The usage patterns of these batteries can lead to rapid degradation [182]. Understanding what LI battery

degradation is, is a key component to increasing the operational lifetime thereof; this will in turn help to accurately predict the failure point and prevent or reduce the risk of thermal runaway [171].

There are generally three external stress factors that influence degradation: temperature, SoC and load profile. The importance of each of these factors varies depending on the chemistry, form factor and historic use conditions, amongst others. These stress factors can influence the underpinning physical degradation processes. In general, temperature is the most significant stress factor [183]. Higher SoC operation accelerates degradation, whereas higher current operation increases the likelihood of failure. These and some other causes are detailed below in Table 7.

Table 7. Causes of degradation in lithium-ion batteries, adapted from [184–192].

Type	Description	Consequence
Over-discharge	When the battery is discharged lower than the recommended DoD voltage. Over discharge leads to over-deintercalation of the LIs in the anode.	Leads to decomposition of the solid electrolyte interface (SEI) and generates CO_2 gasses; recharge allows for new SEI film formation with a different morphology that degrades the electrochemical charge transfer process and increases the internal resistance; Leads to oxidization of the copper collector plates—higher internal resistance and lower capacity; also leads to power losses; Lithium intercalation process causes the electrode structure to expand and contract, forming fine cracks in the structure. This effect is exacerbated when over-deintercalation occurs and leads to increased degradation rate of the electrodes and thus decreases the service life of the battery.
Over-charge	When the battery is left on charge for extended periods of time after reaching full charge status. Leads to excessive heat and eventually thermal runaway.	Thermal runaway causes the anode to overheat and the cathode to release oxygen—poses a potential fire risk; the electrolyte is usually of a flammable substance; this all leads to a potential fire hazard. Excessive heat can also lead to partial shutdown of the separator (explained later in this article), which increases internal resistance, decreases capacity and charge/discharge rate and subsequently decreases service life of the battery.
High charge/ discharge rate	When the battery is either charged or discharged at a rate higher than recommended.	This leads to excessive heat, LLI and lithium plating, all of which decrease the capacity of the battery permanently and can lead to potential fire hazards.
Loss of lithium inventory (LLI)	Loss of usable LIs. Caused by parasitic reactions and continuous SEI growth.	Decrease in LI leads to lower levels of intercalation and less movement of electrons and thus lower energy density.
Loss of active material (LAM)	Structural and mechanical degradation—breakdown of graphite molecular structure, corrosion of copper collector plates. Insertion or intercalation of LIs into the molecular gaps of the graphite. Subsequent insertion (and removal) leads to the breakdown of the graphite structure.	Can trigger a sudden rapid capacity loss, capacity and power fade as result. Quantity of molecular gaps reduces; less lithium can be intercalated; reduces the energy density.
Ohmic resistance increase	Increase in electronic and ionic resistance of a cell. Due to LLI and LAM.	Increases self-discharge—thus decreasing energy density. Also decreases power density due to resistance of power release.

Table 7. *Cont.*

Type	Description	Consequence
Lithium plating or dendrite growth	Lithium deposits onto the anode instead of intercalating during a charge. If the charge current is too high, faster reactions than what can occur are required; if the operating temperature is too low, reaction rate is too slow—both lead to lithium accumulation on the surface of the anode.	Leads to short circuiting between the electrodes, excessive heat and fire hazards, LLI and LAM.

3.3. Ultra-Capacitor Technology

UC have high energy density, low self-discharge and relatively long lifetime, the last of which is affected by operating temperature, applied charge voltage as well as the charge/discharge current [34,193,194]. Their high cycle life can be attributed to the chemical and electrochemical inertness of the compositions of the electrodes and electrolyte. However, this does not exclude UC from degradation, although they are much slower than their battery counterparts. As UC are significantly more expensive than batteries, it is important to understand their degradation characteristics. The degradation of UC is defined through a reduction in equivalent capacity [195]. Studies show that cyclic aging has a much greater effect on the capacitance degradation rate as compared to calendar aging [34,193,194]. It is shown that the degradation is driven primarily by two mechanisms—one related to the degradation of the electrolyte and the other related to the degradation of the electrodes. The first degradation is present for all operating conditions, whereas the second mechanism is generally more predominant under more stringent conditions (increased temperatures and/or operating voltages). It is also found that the degradation due to the first mechanism is significantly slower than that caused by the second mechanism.

UC do not have a hard-failure point with which to express end-of-life. Instead, they are assessed according to a maximum parameter deviation of approximately 20% reduction in capacitance or 100% increase in equivalent series resistance (ESR) [194].

The aging process of UC generally arises from electrical or thermal stress [196,197], which is attributed to external conditions, such as ambient temperature or working parameters [195]. The behaviours that lead to degradation are discussed in Table 8 below.

Table 8. Causes of degradation in ultra-capacitors, adapted from [198–201].

Type	Description	Consequence
Electrochemical reactions	The operating reactions between the electrodes and electrolytes produces solids and gases	Increases internal pressure—leads to electrode cracks; packaging elongation and damages collectors; Blocks pores of electrode—reduces reactive surface area; Blocks separator—disturbs circulation of the ions
Voltage resets	Periodically discharging the UC to a lower voltage than that which is used during operation	Reorganizes the charge distribution within the electrode pores which exposes new aging zones and leads to a significant increase in aging
Uneven charge distribution	Uneven charge current distribution amongst cells due to individual cell degradation levels	Uneven charging of cells leads to overcharging and overheating of certain cells and thus increased degradation of those cells
Overcharging	When too high voltage is applied to the UC for a period of time	Pressure build up occurs inside the UC due to electrolyte decomposition and increased temperature

3.4. Separator Based ESD Degradation

As separators are one of the three main components of the mentioned ESDs [158], it is important to look into how they degrade and how this in turn can affect the operation and degradation of the ESD. These degradation aspects are discussed in Table 9.

Table 9. Causes of degradation in ESD separators, adapted from [202–209].

Consequence	Description	Cause
Shrinkage	Separator shrinks smaller than required size—creates an electrical conduction path between the electrodes—short circuits, service life degradation, higher internal resistance and possible thermal runaway	Excessive operating temperature—High charge/discharge rate; Overcharging
Shutdown effect	Leads to melting/partial melting of the separator pores decreasing the ion conductivity and uniform current distribution. Reduces service life of ESD, reduces charge/discharge rate, can lead to premature failure of ESD	Excessive operating temperature —High charge/discharge rate; Overcharging
Piercing	Decreases integrity of the separator, creates an electrical conduction path between the electrodes—short circuit, reduces service life of ESD	Growth formations on the electrodes—High charge/discharge rate
Stress effect	Cyclic compression and expansion of the separator—leads to a decrease in the integrity of the separator, can cause shrinkage and wrinkles in the separator	Electrode expansion during charge/discharge—Cyclic effect Frequent charge/discharge cycles

3.5. Methods in Combatting/Reducing Degradation

The listed causes of degradation for the different ESDs can be categorized as mechanical (physical) or chemical [207]. For LA, crystal sulfation, increased electrolyte acidity, stratification and water loss are chemical, whilst electrode corrosion, collector warping and separator shutdown, swelling due to increased internal pressure and short-circuiting are mechanical. For LI, SEI reformation, LLI and lithium plating are chemical, and CO_2-gas creation, collector plate oxidization, electrode cracks, thermal runaway, separator shutdown and LAM are mechanical. Finally, for UC, blocked separator/electrode pores and reorganized charge distribution are chemical, whilst cracks, package elongation, damaged collectors, individual cell degradation and internal pressure increases are mechanical.

Generally, if the degradation is chemical, it can possibly (or partially) be reversed. However, this process would require that the battery be exposed to extreme conditions, opposing that of which lead to the degradation, which, in turn, leads to additional degradation as listed in Tables 6–9; if the changes are mechanical, then they are permanent and attempts at reversal will lead to further degradation [210].

The degradation of the above technologies can largely be attributed to user behaviour—overcharging, over-discharging, environmental temperatures, charging too frequently and not charging frequently enough. These types of degradation are very sensitive, so much so that even one occurrence is too many, and as management of these causes would require constant, un-wavered monitoring of the batteries, this is something that cannot be left to the user if optimal usage, performance and cycle life are to be achieved. Thus, to reduce the degradation, these parameters need to be autonomously controlled—this is achieved through the use of a battery management system (BMS), charge controller, HESS or a combination of the three. The function of each will be discussed further below.

3.5.1. Battery Management System

A BMS sets the operation parameters based on suppliers' specifications. A BMS still allows the user to have some user-defined input, but this input is limited within the optimal

supplier specified range [211]. These specifications, based on optimal battery efficiency and use, are generally depth of discharge and maximum voltage [1]. The BMS can also be integrated with the charge controller to ensure the battery is always charged in the correct manner. The correct manner refers to the use of bulk, absorption and trickle charging [212].

If the design specifications and mentioned charging methods are not used, then the battery will experience some, if not all, of the mentioned degradation types [213,214]. This detrimentally affects the health of your battery, decreasing usability, increasing cost and thus decreasing viability [215].

When using batteries for energy storage, a BMS is required to monitor and maintain safe and optimal operating conditions of each battery and, when applicable, each cell [216]. Batteries are dynamic; they constantly operate in and out of their state of equilibrium during charge and discharge cycles—this poses dangerous operating conditions [214]. In addition, even under normal operating conditions, the battery packs will degrade during cycling. This degradation is amplified by user behaviour (as mentioned above) [217].

The goals of a BMS thus include: matching peak power demands, following the load, reducing intermittency, protecting the cells from internal degradation and capacity fade, providing optimal charging patterns, balancing the cells in a battery pack, etc. [1]. The most basic of these goals is to balance state of charge (SoC) across the cells of the battery pack, for this there are three categories: centralized—a single controller with multiple wires connected to the various cells; distributed—a BMS board on each cell with a communication cable between the battery and controller; modular—a few controllers, each controlling a few cells where the controllers communicate with each other. Centralized is economical but least expandable and messy (in terms of the wires); distributed are the most expensive but they are the simplest to implement and the cleanest; modular is a combination of the other two [218].

LA batteries do not have separate cell indicators or measurements—they do not require cell balancing—thus, this aspect of a BMS is lost here [219]. LI technologies, on the other hand, require cell balancing and thermal monitoring of these cells specifically, thus proving the usefulness of this aspect of BMSs. The BMS is therefore primarily used to reduce/prevent unnecessary degradation due to user behaviour (overcharge, undercharge, over-discharge, incorrect charge patterns, etc.) and monitor safety aspects (thermal runaway) [220]. One other very important role of BMSs is to control the charge process; this is discussed later.

3.5.2. Charge Controller

A charge controller regulates the current flowing from the power source into the battery bank to avoid overcharging the batteries [83,221]. There are two variations of charge controllers: pulse width modulation (PWM) and maximum power point tracking (MPPT) [222,223]. PWM accepts the power that is available from the source and adjusts the voltage according to what the battery requires. The battery will only receive the maximum current that the source is rated to supply [224]. As the battery charges, the required voltage will increase and resultantly increase the power used from the source. However, the maximum power of the source will only be utilized if the battery requires a voltage that matches the maximum voltage supply of the source [225]. MPPT acts as a buffer and uses the voltage required by the source to determine the current used according to the maximum power available. Therefore, MPPT will always supply the maximum power available [226].

3.5.3. Hybrid Energy Storage System

Due to the properties of batteries, higher energy density vs. power density, weight, slower recharge, etc., it is very beneficial to combine various energy sources to obtain the best of both (or multiple) worlds from their various properties. By combining multiple energy sources, it is also possible to reduce the accumulative degradation (the usage of each source is reduced per use) [227].

In order to combine energy sources to gain these benefits, careful consideration needs to be taken regarding the energy management of the system—in other words, when to use which source [228]. It is important to control when each source is used, and for what purpose, such that the benefits can actually be achieved and optimized [229]. This can be controlled in a multitude of strategies, known as an energy management strategy (EMS). An EMS is a set of processes that monitor, control and optimize the performance of an energy system [230]. This is mainly achieved through the allocation of the HESS [231]. A basic strategy is achieved through topological control (a strategy referring to the placement of the sources with respect to the load [232])—this can include bi-directional or uni-directional flow of current.

From previous experimentation, A. Townsend et al. [232], the order of the connections can have an effect on the usage of the sources. In the case study, experimentation combined two sources to provide a load using a topological EMS. One test placed both sources before the load and another placed the load between the sources [232]. This strategy does not require any electronic control or switching between the sources, is a very basic EMS and provides a benefit of a less complex, smaller sized and lighter system but does not deliver the most optimal HESS [232].

The main objective of an EMS is to coordinate the power allocation of the independent sources of the HESS [233]. This is generally divided into two categories: rule-based and optimization-based [216]. Both methods create a set of rules and a set of HESS states—the states determine which source is in use and the rules determine which state the HESS should be in. The rules for each state are determined by completed experimentation; they do not vary after implementation. For the rule-based strategy, instantaneous measurements, of the source and load, are used to comply with the rules and determine the HESS state [234,235].

The optimization-based EMS predicts the requirements of the load and adjusts the HESS state according to this prediction. These predictions are based on continued use of the implemented system, thus optimizing through use [236–238]. This method can further be divided into online and offline methods [239]—the latter will develop its own database of information from its own use; online methods use information gathered from a global network containing collections of applications of the implemented system or those similar to it. Online requires a method of connecting to this global platform (cloud), whereas offline requires a large internal memory for continued storage of data. The predictions of this method are continually improved throughout use of the system, thus continuously optimizing the system [229,236,240].

SM. Lukie et al. [241] uses an integrated rule-based meta-heuristic optimization approach for a multi-level EMS of a multi-source EV. A heuristic technique refers to a partial search algorithm, whereas a meta-heuristic technique is more or less accurate solution—it makes certain assumptions initially, which are either local or random. The meta-heuristic technique is used to optimize the split without prior knowledge of the power demand—it makes assumptions according to a local or random online search. For this method, the search space is limited according to pre-set rules and the meta-heuristic technique requires making a few assumptions. Although the latter point allows the approach to find good solutions over a larger search space with less computational effort than other more precise efforts, it still requires these assumptions, thus leading to a solution whose accuracy is dependent on those initial assumptions.

Z. Y. Chen et al. [242] uses a fuzzy logic, rule-based control strategy for a parallel HEV. This EMS uses the initial capacity of the battery and does not take into account the depletion and degradation due to its use.

C. G. Hochgraf et al. [243] uses a flatness control technique (FCT) and fuzzy logic control (FLC) for the EMS. This technique uses a single, general control algorithm in different operating modes, to avoid commutation, and no predictions of system behaviour are made. Once again, the depletion and degradation of the capacity of the battery is not taken into account for this EMS.

H. M. Liu et al. [244] uses a multiple for-loop structure with a pre-set cost function to globally calculate the best EMS. A three-mode rule-based strategy is used to minimize the total consumed energy. This method requires that a pre-set cost function be used, and pre-set rules are used to determine the states of the HESS. These rules are static and do not vary throughout use of the HESS.

J. Cao et al. [245] uses an optimization-based HESS for an electric bus. This EMS utilises FLC, MPC, rule-based controller (RBC) and filtration-based controller (FBC). FLC uses pre-set rules that do not vary throughout the use of the EMS, MPC predicts future trends of use, RBC uses pre-set rules and FBC requires estimates of use—all four of the methods are based on the initial capacities of the source.

H. L. Yu et al. [246] utilizes ESDs of which the current and SOC are maintained within pre-defined limits during operation. The EMS utilizes an MPC and predicts the duty cycle value required for the DC-DC controllers of the battery and capacitor, such that the provided current will equal the required current. This is based on the SOC, voltage and current of the hybrid sources. This optimization-based method predicts the duty cycle requirements based on the initial capacities (SOC range, voltage and current) of the sources.

A. Burke et al. [247] uses an offline optimization-based HESS. This system utilizes MPC and rule-based strategy. A period of future velocity is predicted, and an algorithm is applied to optimize the control strategy accordingly. These velocity predictions are according to the data accumulated for the HESS by the HESS.

J. Y. Shen et al. [248] compares generalized exponentially varying (GEV), artificial neural network (ANN) (time-series forecasting and Markov chain models) and vehicular velocity modelling, when used in an HESS. GEV predicts future velocities. This prediction requires an initial velocity, time-step and exponential coefficient. ANN is accurate in predicting non-linear dynamic behaviour. It can be trained to learn a highly non-linear input/output relationship.

A Markov chain model is accurate for predicted fixed route driving patterns; this is not so much the case with comprehensive driving tasks. Prediction relies on the present state and historical values—the more historical the data the more accurate the prediction. The Markov chain complexity can be increased if more conditions are included, which will resultantly improve accuracy; however, complexity requires more historical data and for the chains to cover all possible input states.

In J. Shen et al. [229], a multi-objective problem is formulated to optimize the power split. This EMS uses dynamic programming, and a neural network (NN) does the power split. This is an online EMS thus requiring the collection of previously obtained results in similar applications.

4. Conclusions

Comparing the various degradation causes for the mentioned ESDs, a few commonalities can be obtained. Over-discharging, over-charging and increased internal resistance (IR) are the three most common causes amongst the ESDs, the first of which is more specific for BESS and not so much for UC. Increases in IR are generally due to all the other causes—electrolyte and active material ionic mobility, separator efficiency, concentration polarisation and temperatures [249]—as the ESD degrades the internal resistance increases, reducing the ability of the ESDs to supply the specified capacity and thus reducing the overall capacity of the ESDs [250].

All of the EMSs discussed in Section 3.5.3 have a pre-determined set switching point—the rules used to determine when, and how, each source is used—that does not vary throughout use of the system. These rules are generally made according to the range of the source and the current requirements of the load. The range of the source(s) is determined by the pre-defined and initial SOC, DoD, energy density and power density ratings. All of these ratings change during each use and throughout the sources' lifetime—these changes are not included in the initial design, or continued optimization, of the system [142].

All of these systems and methods are aimed at reducing the effects and causes of the mentioned degradation; none look into adjusting use dynamically to reduce further degradation. For example, it is a well-known fact that the capacity drops as the used cycles increase, but the battery is still utilised within the original full-health parameters.

A basic BMS will control only the battery packs to meet the load requirements; when intelligent control is integrated, BMSs can reduce the causes of degradation, providing more optimal performance and cycle life. There exist many different variations of BMSs and intricate control algorithms that help prevent or reduce the behaviours that can accelerate degradation of the battery. Herein lies the dilemma—these systems are designed to reduce the cause of degradation through better utilization of the battery. However, one largely overlooked factor is that the battery continues to be used according to its original "full-health" specifications. Figure 3 of P. Zhang et al. [8] and Figure 11 of V. Sedlakova et al. [9] illustrate the well-known fact that battery capacity decreases as more cycles are utilized—the degradation being discussed—yet the battery is still used according to the original capacity.

If discharge capacity is decreasing, essentially C-rate should be adjusted, accordingly; the maximum voltage drops. Thus, this value should be adjusted to avoid over-charging as charging range has dropped; essentially power density is also decreasing and therefore the surge values should be reduced. As the cycles of the battery are the optimal range within which the battery should charge and discharge to achieve the best longevity from the capacity, if the battery maximum voltage drops, then essentially only a portion of the cycle will be used (if an adjustment is made to this parameter in the BMS). This dynamic adjustment or alteration can lead to two results: an improvement in cycle life and a reduction in overcharge degradation.

Battery and UC degradation is a given; regardless of how well it is used, it will degrade. Thus, the proposal is to measure the degradation, dynamically and continuously, and include it in the parameters of the BMS and charge controller. Previous studies look into methods of reducing the causes of degradation, but there are few studies that look into the increase in said degradation when battery use is continued according to its initial "full health" parameters, or the adjustment of the parameters as the battery degrades.

Author Contributions: Conceptualization and writing, original draft preparation, editing, A.T.; Conceptualization, review, editing, supervision, R.G. All authors have read and agreed to the published version of the manuscript.

Funding: This research received no external funding.

Institutional Review Board Statement: Not applicable.

Informed Consent Statement: Not applicable.

Data Availability Statement: Not applicable.

Conflicts of Interest: The authors declare no conflict of interest.

References

1. Lawder, M.T.; Suthar, B.; Northrop, P.W.C.; De, S.; Hoff, C.M.; Leitermann, O.; Crow, M.L.; Santhanagopalan, S.; Subramanian, V.R. Battery Energy Storage System (BESS) and Battery Management System (BMS) for Grid-Scale Applications. *Proc. IEEE* **2014**, *102*, 1014–1030. [CrossRef]
2. Cagnano, A.; De Tuglie, E.; Gibilisco, P. Assessment and Control of Microgrid Impacts on Distribution Networks by Using Experimental Tests. *IEEE Trans. Ind. Appl.* **2019**, *55*, 7157–7164. [CrossRef]
3. Sarbu, I.; Sebarchievici, C. A Comprehensive Review of Thermal Energy Storage. *Sustainability* **2018**, *10*, 191. [CrossRef]
4. Ball, M.; Weeda, M. The Hydrogen Economy—Vision or Reality? In *Compendium of Hydrogen Energy*; Elsevier: Amsterdam, The Netherlands, 2016; pp. 237–266.
5. Zsiborács, H.; Baranyai, N.H.; Vincze, A.; Zentkó, L.; Birkner, Z.; Máté, K.; Pintér, G. Intermittent Renewable Energy Sources: The Role of Energy Storage in the European Power System of 2040. *Electronics* **2019**, *8*, 729. [CrossRef]
6. Asiaban, S.; Kayedpour, N.; Samani, A.E.; Bozalakov, D.; De Kooning, J.D.M.; Crevecoeur, G.; Vandevelde, L. Wind and Solar Intermittency and the Associated Integration Challenges: A Comprehensive Review Including the Status in the Belgian Power System. *Energies* **2021**, *14*, 2630. [CrossRef]

7. Neill, S.P.; Hashemi, M.R. Tidal Energy. In *Fundamentals of Ocean Renewable Energy*; Elsevier: Amsterdam, The Netherlands, 2018; pp. 47–81.
8. Suchet, D.; Jeantet, A.; Elghozi, T.; Jehl, Z. Defining and Quantifying Intermittency in the Power Sector. *Energies* **2020**, *13*, 3366. [CrossRef]
9. Notton, G.; Nivet, M.-L.; Voyant, C.; Paoli, C.; Darras, C.; Motte, F.; Fouilloy, A. Intermittent and Stochastic Character of Renewable Energy Sources: Consequences, Cost of Intermittence and Benefit of Forecasting. *Renew. Sustain. Energy Rev.* **2018**, *87*, 96–105. [CrossRef]
10. Platt, G.; Paevere, P.; Higgins, A.; Grozev, G. Electric Vehicles. In *Distributed Generation and Its Implications for the Utility Industry*; Elsevier: Amsterdam, The Netherlands, 2014; pp. 335–355.
11. Hasanuzzaman, M.; Kumar, L. Energy Supply. In *Energy for Sustainable Development*; Elsevier: Amsterdam, The Netherlands, 2020; pp. 89–104.
12. Abdi, H.; Mohammadi-ivatloo, B.; Javadi, S.; Khodaei, A.R.; Dehnavi, E. Energy Storage Systems. In *Distributed Generation Systems*; Elsevier: Amsterdam, The Netherlands, 2017; pp. 333–368.
13. Aktaş, A.; Kirçiçek, Y. Hybrid Energy Storage and Innovative Storage Technologies. In *Solar Hybrid Systems*; Elsevier: Amsterdam, The Netherlands, 2021; pp. 139–152.
14. Zafirakis, D.P. Overview of Energy Storage Technologies for Renewable Energy Systems. In *Stand-Alone and Hybrid Wind Energy Systems*; Elsevier: Amsterdam, The Netherlands, 2010; pp. 29–80.
15. Poullikkas, A. A Comparative Overview of Large-Scale Battery Systems for Electricity Storage. *Renew. Sustain. Energy Rev.* **2013**, *27*, 778–788. [CrossRef]
16. Panchabikesan, K.; Mastani Joybari, M.; Haghighat, F.; Eicker, U.; Ramalingam, V. Analogy between Thermal, Mechanical, and Electrical Energy Storage Systems. In *Encyclopedia of Energy Storage*; Elsevier: Amsterdam, The Netherlands, 2022; pp. 315–328.
17. Ding, K.; Zhi, J. Wind Power Peak-Valley Regulation and Frequency Control Technology. In *Large-Scale Wind Power Grid Integration*; Elsevier: Amsterdam, The Netherlands, 2016; pp. 211–232.
18. Abdin, Z.; Khalilpour, K.R. Single and Polystorage Technologies for Renewable-Based Hybrid Energy Systems. In *Polygeneration with Polystorage for Chemical and Energy Hubs*; Elsevier: Amsterdam, The Netherlands, 2019; pp. 77–131.
19. Semadeni, M. Storage of Energy, Overview. In *Encyclopedia of Energy*; Elsevier: Amsterdam, The Netherlands, 2004; pp. 719–738.
20. Stadler, I.; Sterner, M. Urban Energy Storage and Sector Coupling. In *Urban Energy Transition*; Elsevier: Amsterdam, The Netherlands, 2018; pp. 225–244.
21. Jana, A.; Paul, R.; Roy, A.K. Architectural Design and Promises of Carbon Materials for Energy Conversion and Storage: In Laboratory and Industry. In *Carbon Based Nanomaterials for Advanced Thermal and Electrochemical Energy Storage and Conversion*; Elsevier: Amsterdam, The Netherlands, 2019; pp. 25–61.
22. Revankar, S.T. Chemical Energy Storage. In *Storage and Hybridization of Nuclear Energy*; Elsevier: Amsterdam, The Netherlands, 2019; pp. 177–227.
23. Divya, K.C.; Østergaard, J. Battery Energy Storage Technology for Power Systems—An Overview. *Electr. Power Syst. Res.* **2009**, *79*, 511–520. [CrossRef]
24. Townsend, A.; Jiya, I.N.; Martinson, C.; Bessarabov, D.; Gouws, R. A Comprehensive Review of Energy Sources for Unmanned Aerial Vehicles, Their Shortfalls and Opportunities for Improvements. *Heliyon* **2020**, *6*, 1–22. [CrossRef]
25. Cano, Z.P.; Banham, D.; Ye, S.; Hintennach, A.; Lu, J.; Fowler, M.; Chen, Z. Batteries and Fuel Cells for Emerging Electric Vehicle Markets. *Nat. Energy* **2018**, *3*, 279–289. [CrossRef]
26. Srinivasan, S. *Fuel Cells*; Springer: Boston, MA, USA, 2006; ISBN 978-0-387-25116-5. [CrossRef]
27. Williamson, S.S.; Cassani, P.A.; Lukic, S.; Blunier, B. Energy Storage. In *Power Electronics Handbook*; Elsevier: Amsterdam, The Netherlands, 2011; pp. 1331–1356.
28. Qi, Z.; Koenig, G.M. Review Article: Flow Battery Systems with Solid Electroactive Materials. *J. Vac. Sci. Technol. B Nanotechnol. Microelectron. Mater. Process. Meas. Phenom.* **2017**, *35*, 040801. [CrossRef]
29. Guan, W.; Huang, X. A Modular Active Balancing Circuit for Redox Flow Battery Applied in Energy Storage System. *IEEE Access* **2021**, *9*, 127548–127558. [CrossRef]
30. Motapon, S.N.; Lachance, E.; Dessaint, L.-A.; Al-Haddad, K. A Generic Cycle Life Model for Lithium-Ion Batteries Based on Fatigue Theory and Equivalent Cycle Counting. *IEEE Open J. Ind. Electron. Soc.* **2020**, *1*, 207–217. [CrossRef]
31. Zhang, D.; Dey, S.; Perez, H.E.; Moura, S.J. Real-Time Capacity Estimation of Lithium-Ion Batteries Utilizing Thermal Dynamics. *IEEE Trans. Control Syst. Technol.* **2020**, *28*, 992–1000. [CrossRef]
32. Barré, A.; Deguilhem, B.; Grolleau, S.; Gérard, M.; Suard, F.; Riu, D. A Review on Lithium-Ion Battery Ageing Mechanisms and Estimations for Automotive Applications. *J. Power Sources* **2013**, *241*, 680–689. [CrossRef]
33. Zhang, P.; Liang, J.; Zhang, F. An Overview of Different Approaches for Battery Lifetime Prediction. *IOP Conf. Ser. Mater. Sci. Eng.* **2017**, *199*, 012134. [CrossRef]
34. Sedlakova, V.; Sikula, J.; Majzner, J.; Sedlak, P.; Kuparowitz, T.; Buergler, B.; Vasina, P. Supercapacitor Degradation Assesment by Power Cycling and Calendar Life Tests. *Metrol. Meas. Syst.* **2016**, *23*, 345–358. [CrossRef]
35. Mendis, N.; Muttaqi, K.M.; Perera, S. Management of Low- and High-Frequency Power Components in Demand-Generation Fluctuations of a DFIG-Based Wind-Dominated RAPS System Using Hybrid Energy Storage. *IEEE Trans. Ind. Appl.* **2014**, *50*, 2258–2268. [CrossRef]

36. Sathishkumar, R.; Kollimalla, S.K.; Mishra, M.K. Dynamic Energy Management of Micro Grids Using Battery Super Capacitor Combined Storage. In Proceedings of the 2012 Annual IEEE India Conference (INDICON), Kochi, India, 7–9 December 2012; IEEE: New York, NY, USA, 2012; pp. 1078–1083.
37. Basic, H.; Pandzic, H.; Miletic, M.; Pavic, I. Experimental Testing and Evaluation of Lithium-Ion Battery Cells for a Special-Purpose Electric Vacuum Sweeper Vehicle. *IEEE Access* **2020**, *8*, 216308–216319. [CrossRef]
38. McKeon, B.B.; Furukawa, J.; Fenstermacher, S. Advanced Lead–Acid Batteries and the Development of Grid-Scale Energy Storage Systems. *Proc. IEEE* **2014**, *102*, 951–963. [CrossRef]
39. Al-Haj Hussein, A.; Batarseh, I. A Review of Charging Algorithms for Nickel and Lithium Battery Chargers. *IEEE Trans. Veh. Technol.* **2011**, *60*, 830–838. [CrossRef]
40. da Cunha, A.B.; de Almeida, B.R.; da Silva, D.C. Remaining Capacity Measurement and Analysis of Alkaline Batteries for Wireless Sensor Nodes. *IEEE Trans. Instrum. Meas.* **2009**, *58*, 1816–1822. [CrossRef]
41. Kupsch, C.; Weik, D.; Feierabend, L.; Nauber, R.; Buttner, L.; Czarske, J. Vector Flow Imaging of a Highly Laden Suspension in a Zinc-Air Flow Battery Model. *IEEE Trans. Ultrason. Ferroelectr. Freq. Control* **2019**, *66*, 761–771. [CrossRef]
42. Al-Humaid, Y.M.; Khan, K.A.; Abdulgalil, M.A.; Khalid, M. Two-Stage Stochastic Optimization of Sodium-Sulfur Energy Storage Technology in Hybrid Renewable Power Systems. *IEEE Access* **2021**, *9*, 162962–162972. [CrossRef]
43. Aktaş, A.; Kirçiçek, Y. Solar Hybrid Systems and Energy Storage Systems. In *Solar Hybrid Systems*; Elsevier: Amsterdam, The Netherlands, 2021; pp. 87–125.
44. Battery University BU-201: How Does the Lead Acid Battery Work? Available online: https://batteryuniversity.com/article/bu-201-how-does-the-lead-acid-battery-work (accessed on 22 April 2022).
45. Dhundhara, S.; Verma, Y.P.; Williams, A. Techno-Economic Analysis of the Lithium-Ion and Lead-Acid Battery in Microgrid Systems. *Energy Convers. Manag.* **2018**, *177*, 122–142. [CrossRef]
46. Jaiswal, A. Lithium-Ion Battery Based Renewable Energy Solution for off-Grid Electricity: A Techno-Economic Analysis. *Renew. Sustain. Energy Rev.* **2017**, *72*, 922–934. [CrossRef]
47. Eldeeb, H.H.; Elsayed, A.T.; Lashway, C.R.; Mohammed, O. Hybrid Energy Storage Sizing and Power Splitting Optimization for Plug-In Electric Vehicles. *IEEE Trans. Ind. Appl.* **2019**, *55*, 2252–2262. [CrossRef]
48. Diaz, J.; Martin-Ramos, J.A.; Pernia, A.M.; Nuno, F.; Linera, F.F. Intelligent and Universal Fast Charger for Ni-Cd and Ni-MH Batteries in Portable Applications. *IEEE Trans. Ind. Electron.* **2004**, *51*, 857–863. [CrossRef]
49. Buchmann, I. *Batteries in a Portable World: A Handbook on Rechargeable Batteries for Non-Engineers*, 4th ed.; CADEX: Richmond, BC, Canada, 2017; ISBN 978-0968211847.
50. Lim, M.B.; Lambert, T.N.; Chalamala, B.R. Rechargeable Alkaline Zinc–Manganese Oxide Batteries for Grid Storage: Mechanisms, Challenges and Developments. *Mater. Sci. Eng. R Rep.* **2021**, *143*, 100593. [CrossRef]
51. De Angelis, V.; Yadav, G.; Huang, J.; Couzis, A.; Banerjee, S. Rechargeable Zn-MnO_2 Batteries for Utility Load Management and Renewable Integration. In Proceedings of the 2018 International Symposium on Power Electronics, Electrical Drives, Automation and Motion (SPEEDAM), Amalfi, Italy, 20 June 2018; IEEE: New York, NY, USA, 2018; pp. 50–54.
52. Salkind, A.J.; Klein, M. Batteries, Alkaline Secondary Cells. In *Kirk-Othmer Encyclopedia of Chemical Technology*; John Wiley & Sons, Inc.: Hoboken, NJ, USA, 2000.
53. Olabi, A.G.; Sayed, E.T.; Wilberforce, T.; Jamal, A.; Alami, A.H.; Elsaid, K.; Rahman, S.M.A.; Shah, S.K.; Abdelkareem, M.A. Metal-Air Batteries—A Review. *Energies* **2021**, *14*, 7373. [CrossRef]
54. Fan, X.; Liu, B.; Liu, J.; Ding, J.; Han, X.; Deng, Y.; Lv, X.; Xie, Y.; Chen, B.; Hu, W.; et al. Battery Technologies for Grid-Level Large-Scale Electrical Energy Storage. *Trans. Tianjin Univ.* **2020**, *26*, 92–103. [CrossRef]
55. Chawla, N.; Safa, M. Sodium Batteries: A Review on Sodium-Sulfur and Sodium-Air Batteries. *Electronics* **2019**, *8*, 1201. [CrossRef]
56. Chen, H.; Cong, T.N.; Yang, W.; Tan, C.; Li, Y.; Ding, Y. Progress in Electrical Energy Storage System: A Critical Review. *Prog. Nat. Sci.* **2009**, *19*, 291–312. [CrossRef]
57. Doetsch, C.; Pohlig, A. The Use of Flow Batteries in Storing Electricity for National Grids. In *Future Energy*; Elsevier: Amsterdam, The Netherlands, 2020; pp. 263–277.
58. Zhang, D.; Liu, Q.; Li, Y. Design of Flow Battery. In *Reactor and Process Design in Sustainable Energy Technology*; Elsevier: Amsterdam, The Netherlands, 2014; pp. 61–97.
59. Chalamala, B.R.; Soundappan, T.; Fisher, G.R.; Anstey, M.R.; Viswanathan, V.V.; Perry, M.L. Redox Flow Batteries: An Engineering Perspective. *Proc. IEEE* **2014**, *102*, 976–999. [CrossRef]
60. Ferrari, J. Energy Storage and Conversion. In *Electric Utility Resource Planning*; Elsevier: Amsterdam, The Netherlands, 2021; pp. 73–107.
61. Nguyen, T.A.; Crow, M.L.; Elmore, A.C. Optimal Sizing of a Vanadium Redox Battery System for Microgrid Systems. *IEEE Trans. Sustain. Energy* **2015**, *6*, 729–737. [CrossRef]
62. Bahramirad, S.; Reder, W.; Khodaei, A. Reliability-Constrained Optimal Sizing of Energy Storage System in a Microgrid. *IEEE Trans. Smart Grid* **2012**, *3*, 2056–2062. [CrossRef]
63. Brady, R.N. Internal Combustion (Gasoline and Diesel) Engines. In *Reference Module in Earth Systems and Environmental Sciences*; Elsevier: Amsterdam, The Netherlands, 2013.
64. Mahapatra, M.K.; Singh, P. Fuel Cells. In *Future Energy*; Elsevier: Amsterdam, The Netherlands, 2014; pp. 511–547.

65. Bharadwaj, S.R.; Varma, S.; Wani, B.N. Electroceramics for Fuel Cells, Batteries and Sensors. In *Functional Materials*; Elsevier: Amsterdam, The Netherlands, 2012; pp. 639–674.
66. Campanari, S.; Guandalini, G. Fuel Cells: Opportunities and Challenges. In *Studies in Surface Science and Catalysis*; Elsevier: Amsterdam, The Netherlands, 2020; pp. 335–358.
67. Pollet, B.G.; Staffell, I.; Shang, J.L.; Molkov, V. Fuel-Cell (Hydrogen) Electric Hybrid Vehicles. In *Alternative Fuels and Advanced Vehicle Technologies for Improved Environmental Performance*; Elsevier: Amsterdam, The Netherlands, 2014; pp. 685–735.
68. Dincer, I.; Siddiqui, O. Fundamentals. In *Ammonia Fuel Cells*; Elsevier: Amsterdam, The Netherlands, 2020; pp. 13–32.
69. Coralli, A.; Sarruf, B.J.M.; de Miranda, P.E.V.; Osmieri, L.; Specchia, S.; Minh, N.Q. Fuel Cells. In *Science and Engineering of Hydrogen-Based Energy Technologies*; Elsevier: Amsterdam, The Netherlands, 2019; pp. 39–122.
70. Hebling, C.; Rochlitz, L.; Aicher, T. Micro-Fuel Cells. In *Comprehensive Microsystems*; Elsevier: Amsterdam, The Netherlands, 2008; pp. 613–634.
71. Thangavelautham, J. Degradation in PEM Fuel Cells and Mitigation Strategies Using System Design and Control. In *Proton Exchange Membrane Fuel Cell*; InTech: London, UK, 2018.
72. Surabattula, Y.; Balaji, R.; Rajalakshmi, N.; Prakash, K.A. First and Second Law of Thermodynamics—Analysis for Fuel Cells. In *Encyclopedia of Energy Storage*; Elsevier: Amsterdam, The Netherlands, 2022; pp. 307–314.
73. Popov, S.P.; Baldynov, O.A. Evaluation of Energy Efficiency of the Long Distance Energy Transport Systems for Renewable Energy. *E3S Web Conf.* **2019**, *114*, 02003. [CrossRef]
74. Behling, N.H. Fuel Cells and the Challenges Ahead. In *Fuel Cells*; Elsevier: Amsterdam, The Netherlands, 2013; pp. 7–36.
75. Russel Rhodes Explosive Lessons in Hydrogen Saftey. Available online: https://www.nasa.gov/pdf/513855main_ASK_41s_explosive.pdf (accessed on 22 June 2022).
76. Coddet, P.; Pera, M.-C.; Candusso, D.; Hissel, D. Study of Proton Exchange Membrane Fuel Cell Safety Procedures in Case of Emergency Shutdown. In Proceedings of the 2007 IEEE International Symposium on Industrial Electronics, Vigo, Spain, 4–7 June 2007; IEEE: New York, NY, USA, 2007; pp. 725–730.
77. Fathima, A.H.; Palanisamy, K. Renewable Systems. In *Hybrid-Renewable Energy Systems in Microgrids*; Elsevier: Amsterdam, The Netherlands, 2018; pp. 147–164.
78. Yoomak, S.; Ngaopitakkul, A. Feasibility Analysis of Different Energy Storage Systems for Solar Road Lighting Systems. *IEEE Access* **2019**, *7*, 101992–102001. [CrossRef]
79. Akinyele, D.; Belikov, J.; Levron, Y. Battery Storage Technologies for Electrical Applications: Impact in Stand-Alone Photovoltaic Systems. *Energies* **2017**, *10*, 1760. [CrossRef]
80. Linden, D.; Reddy, T.B. *Handbook of Batteries*, 3rd ed.; McGraw-Hill: New York, NY, USA, 2002. Available online: https://en.wikipedia.org/wiki/Special:BookSources/0-07-135978-8 (accessed on 4 April 2022).
81. Schwimmbeck, S.; Schroer, P.; Buchner, Q.; Herzog, H.-G. Modeling the Dynamic Behavior of 12V AGM Batteries and Its Degradation. In Proceedings of the 2019 IEEE Vehicle Power and Propulsion Conference (VPPC), Hanoi, Vietnam, 14–17 October 2019; IEEE: New York, NY, USA, 2019; pp. 1–6.
82. May, G.J.; Davidson, A.; Monahov, B. Lead Batteries for Utility Energy Storage: A Review. *J. Energy Storage* **2018**, *15*, 145–157. [CrossRef]
83. Satpathy, R.; Pamuru, V. Off-Grid Solar Photovoltaic Systems. In *Solar PV Power*; Elsevier: Amsterdam, The Netherlands, 2021; pp. 267–315.
84. Pascoe, P.E.; Anbuky, A.H. VRLA Battery Discharge Reserve Time Estimation. *IEEE Trans. Power Electron.* **2004**, *19*, 1515–1522. [CrossRef]
85. Torabi, F.; Ahmadi, P. Lead–Acid Batteries. In *Simulation of Battery Systems*; Elsevier: Amsterdam, The Netherlands, 2020; pp. 149–215.
86. Jie, W.; Hua, L.; Peijie, C.; Deyu, Q.; Shan, L. Design of Energy Storage System Using Retired Valve Regulated Lead Acid (VRLA) Batteries in Substations. In Proceedings of the 2019 IEEE Conference on Energy Conversion (CENCON), Yogyakarta, Indonesia, 16–17 October 2019; IEEE: New York, NY, USA, 2019; pp. 132–136.
87. Spiers, D. Batteries in PV Systems. In *McEvoy's Handbook of Photovoltaics*; Elsevier: Amsterdam, The Netherlands, 2018; pp. 789–843.
88. Bonduelle, G.; Muneret, X. VRLA Batteries in Telecom Application: AGM or Gel? In Proceedings of the TELESCON 2000 Third International Telecommunications Energy Special Conference (IEEE Cat. No.00EX424), Dresden, Germany, 10 May 2000; VDE-Verlag: Berlin, Germany; pp. 75–79.
89. Mahlia, T.M.I.; Saktisahdan, T.J.; Jannifar, A.; Hasan, M.H.; Matseelar, H.S.C. A Review of Available Methods and Development on Energy Storage; Technology Update. *Renew. Sustain. Energy Rev.* **2014**, *33*, 532–545. [CrossRef]
90. Trojan J200-RE Deep Cycle Flooded/Advanced Lead Acid Battery. Available online: http://www.trojanbattery.com/pdf/J200-RE_Trojan_Data_Sheets.pdf (accessed on 18 May 2022).
91. Components, R. FG20201 Lead Acid Battery-12 V, 2 Ah. Available online: https://za.rs-online.com/web/p/lead-acid-batteries/8431308/ (accessed on 18 May 2020).
92. Renogy Deep Cycle AGM Battery 12 V 200 Ah. Available online: https://www.renogy.com/content/RNG-BATT-AGM12-200/AGM200-Datasheet.pdf (accessed on 18 May 2022).

93. Kuang, X.; Li, X.; Li, S.; Xiang, J.; Wang, X. Silicon Nanoparticles Within the Carbonized SU-8 Cages as A Micro Lithium-Ion Battery Anode. *J. Microelectromechanical Syst.* **2018**, *27*, 201–209. [CrossRef]
94. Turgeman, M.; Wineman-Fisher, V.; Malchik, F.; Saha, A.; Bergman, G.; Gavriel, B.; Penki, T.R.; Nimkar, A.; Baranauskaite, V.; Aviv, H.; et al. A Cost-Effective Water-in-Salt Electrolyte Enables Highly Stable Operation of a 2.15-V Aqueous Lithium-Ion Battery. *Cell Rep. Phys. Sci.* **2022**, *3*, 100688. [CrossRef]
95. Xiong, R.; Tian, J.; Mu, H.; Wang, C. A Systematic Model-Based Degradation Behavior Recognition and Health Monitoring Method for Lithium-Ion Batteries. *Appl. Energy* **2017**, *207*, 372–383. [CrossRef]
96. Daud, M.Z.; Mohamed, A.; Hannan, M.A. A Novel Coordinated Control Strategy Considering Power Smoothing for a Hybrid Photovoltaic/Battery Energy Storage System. *J. Cent. South Univ.* **2016**, *23*, 394–404. [CrossRef]
97. Kim, H.; Lee, K.; Kim, S.; Kim, Y. Fluorination of Free Lithium Residues on the Surface of Lithium Nickel Cobalt Aluminum Oxide Cathode Materials for Lithium Ion Batteries. *Mater. Des.* **2016**, *100*, 175–179. [CrossRef]
98. Cui, Y.; Mahmoud, M.M.; Rohde, M.; Ziebert, C.; Seifert, H.J. Thermal and Ionic Conductivity Studies of Lithium Aluminum Germanium Phosphate Solid-State Electrolyte. *Solid State Ion.* **2016**, *289*, 125–132. [CrossRef]
99. Zhao, C.; Yin, H.; Ma, C. Quantitative Evaluation of $LiFePO_4$ Battery Cycle Life Improvement Using Ultracapacitors. *IEEE Trans. Power Electron.* **2016**, *31*, 3989–3993. [CrossRef]
100. Tarascon, J.-M.; Recham, N.; Armand, M.; Chotard, J.-N.; Barpanda, P.; Walker, W.; Dupont, L. Hunting for Better Li-Based Electrode Materials via Low Temperature Inorganic Synthesis. *Chem. Mater.* **2010**, *22*, 724–739. [CrossRef]
101. Kennedy, B.; Patterson, D.; Camilleri, S. Use of Lithium-Ion Batteries in Electric Vehicles. *J. Power Sources* **2000**, *90*, 156–162. [CrossRef]
102. Omar, N.; Verbrugge, B.; Mulder, G.; Van den Bossche, P.; Van Mierlo, J.; Daowd, M.; Dhaens, M.; Pauwels, S. Evaluation of Performance Characteristics of Various Lithium-Ion Batteries for Use in BEV Application. In Proceedings of the 2010 IEEE Vehicle Power and Propulsion Conference, Lille, France, 1–3 September 2010; IEEE: New York, NY, USA, 2010; pp. 1–6.
103. Meng, J.; Luo, G.; Gao, F. Lithium Polymer Battery State-of-Charge Estimation Based on Adaptive Unscented Kalman Filter and Support Vector Machine. *IEEE Trans. Power Electron.* **2016**, *31*, 2226–2238. [CrossRef]
104. Kim, T.; Qiao, W.; Qu, L. Power Electronics-Enabled Self-X Multicell Batteries: A Design Toward Smart Batteries. *IEEE Trans. Power Electron.* **2012**, *27*, 4723–4733. [CrossRef]
105. Li, Z.; Li, J.; Zhao, Y.; Yang, K.; Gao, F.; Li, X. Influence of Cooling Mode on the Electrochemical Properties of $Li_4Ti_5O_{12}$ Anode Materials for Lithium-Ion Batteries. *Ionics* **2016**, *22*, 789–795. [CrossRef]
106. Liu, W.; Wang, Y.; Jia, X.; Xia, B. The Characterization of Lithium Titanate Microspheres Synthesized by a Hydrothermal Method. *J. Chem.* **2013**, *2013*, 497654. [CrossRef]
107. Llinas, J.P.; Fairbrother, A.; Borin Barin, G.; Shi, W.; Lee, K.; Wu, S.; Yong Choi, B.; Braganza, R.; Lear, J.; Kau, N.; et al. Short-Channel Field-Effect Transistors with 9-Atom and 13-Atom Wide Graphene Nanoribbons. *Nat. Commun.* **2017**, *8*, 633. [CrossRef]
108. Zhang, Z.; Zhang, Q.; Chen, Y.; Bao, J.; Zhou, X.; Xie, Z.; Wei, J.; Zhou, Z. The First Introduction of Graphene to Rechargeable Li-CO_2 Batteries. *Angew. Chem.* **2015**, *127*, 6650–6653. [CrossRef]
109. Lee, J.H.; Yoon, C.S.; Hwang, J.-Y.; Kim, S.-J.; Maglia, F.; Lamp, P.; Myung, S.-T.; Sun, Y.-K. High-Energy-Density Lithium-Ion Battery Using a Carbon-Nanotube–Si Composite Anode and a Compositionally Graded $Li[Ni_{0.85}Co_{0.05}Mn_{0.10}]O_2$ Cathode. *Energy Environ. Sci.* **2016**, *9*, 2152–2158. [CrossRef]
110. Quartarone, E.; Dall'Asta, V.; Resmini, A.; Tealdi, C.; Tredici, I.G.; Tamburini, U.A.; Mustarelli, P. Graphite-Coated ZnO Nanosheets as High-Capacity, Highly Stable, and Binder-Free Anodes for Lithium-Ion Batteries. *J. Power Sources* **2016**, *320*, 314–321. [CrossRef]
111. Huang, Q.; Yang, J.; Ng, C.B.; Jia, C.; Wang, Q. A Redox Flow Lithium Battery Based on the Redox Targeting Reactions between $LiFePO_4$ and Iodide. *Energy Environ. Sci.* **2016**, *9*, 917–921. [CrossRef]
112. Gong, H.; Xue, H.; Wang, T.; He, J. In-Situ Synthesis of Monodisperse Micro-Nanospherical $LiFePO_4$/Carbon Cathode Composites for Lithium-Ion Batteries. *J. Power Sources* **2016**, *318*, 220–227. [CrossRef]
113. Thackeray, M.M.; Thomas, J.O.; Whittingham, M.S. Science and Applications of Mixed Conductors for Lithium Batteries. *MRS Bull.* **2000**, *25*, 39–46. [CrossRef]
114. Omar, N.; Monem, M.A.; Firouz, Y.; Salminen, J.; Smekens, J.; Hegazy, O.; Gaulous, H.; Mulder, G.; Van den Bossche, P.; Coosemans, T.; et al. Lithium Iron Phosphate Based Battery–Assessment of the Aging Parameters and Development of Cycle Life Model. *Appl. Energy* **2014**, *113*, 1575–1585. [CrossRef]
115. Häggström, F.; Delsing, J. IoT Energy Storage-A Forecast. *Energy Harvest. Syst.* **2018**, *5*, 43–51. [CrossRef]
116. Bueno, P.R. Nanoscale Origins of Super-Capacitance Phenomena. *J. Power Sources* **2019**, *414*, 420–434. [CrossRef]
117. Gupta, S.S.; Islam, M.R.; Pradeep, T. Capacitive Deionization (CDI): An Alternative Cost-Efficient Desalination Technique. In *Advances in Water Purification Techniques*; Elsevier: Amsterdam, The Netherlands, 2019; pp. 165–202.
118. Shafiei, N.; Nasrollahzadeh, M.; Hegde, G. Biopolymer-Based (Nano)Materials for Supercapacitor Applications. In *Biopolymer-Based Metal Nanoparticle Chemistry for Sustainable Applications*; Elsevier: Amsterdam, The Netherlands, 2021; pp. 609–671.
119. Grahame, D.C. The Electrical Double Layer and the Theory of Electrocapillarity. *Chem. Rev.* **1947**, *41*, 441–501. [CrossRef]
120. Ellenbogen, J.C. *Supercapacitors: A Brief Overview*; MITRE: McLean, VA, USA, 2006.
121. Helmholtz, H. Ueber Einige Gesetze Der Vertheilung Elektrischer Ströme in Körperlichen Leitern Mit Anwendung Auf Die Thierisch-Elektrischen Versuche. *Ann. Der Phys. Und Chem.* **1853**, *165*, 211–233. [CrossRef]

122. Frackowiak, E.; Jurewicz, K.; Delpeux, S.; Béguin, F. Nanotubular Materials for Supercapacitors. *J. Power Sources* **2001**, *97–98*, 822–825. [CrossRef]
123. Conway, B.E.; Birss, V.; Wojtowicz, J. The Role and Utilization of Pseudocapacitance for Energy Storage by Supercapacitors. *J. Power Sources* **1997**, *66*, 1–14. [CrossRef]
124. Conway, B.E. Transition from "Supercapacitor" to "Battery" Behavior in Electrochemical Energy Storage. *J. Electrochem. Soc.* **1991**, *138*, 1539–1548. [CrossRef]
125. Simon, P.; Burke, A. Nanostructured Carbons: Double-Layer Capacitance and More. *Electrochem. Soc. Interface* **2008**, *17*, 38–43. [CrossRef]
126. Liu, Y.; Jiang, S.P.; Shao, Z. Intercalation Pseudocapacitance in Electrochemical Energy Storage: Recent Advances in Fundamental Understanding and Materials Development. *Mater. Today Adv.* **2020**, *7*, 100072. [CrossRef]
127. Yoong, M.; Gan, Y.; Gan, G.; Leong, C.; Phuan, Z.; Cheah, B.; Chew, K. Studies of Regenerative Braking in Electric Vehicle. In Proceedings of the 2010 IEEE Conference on Sustainable Utilization and Development in Engineering and Technology, Kuala Lumpur, Malaysia, 20–21 November 2010; IEEE: New York, NY, USA, 2010; pp. 40–45.
128. Camara, M.B.; Gualous, H.; Gustin, F.; Berthon, A. Design and New Control of DC/DC Converters to Share Energy between Supercapacitors and Batteries in Hybrid Vehicles. *IEEE Trans. Veh. Technol.* **2008**, *57*, 2721–2735. [CrossRef]
129. Worsley, M.A.; Baumann, T.F. Carbon Aerogels. In *Handbook of Sol-Gel Science and Technology*; Springer International Publishing: Cham, Switzerland, 2016; pp. 1–36.
130. Najib, S.; Erdem, E. Current Progress Achieved in Novel Materials for Supercapacitor Electrodes: Mini Review. *Nanoscale Adv.* **2019**, *1*, 2817–2827. [CrossRef]
131. Lazarov, V.; Francois, B.; Kanchev, H.; Zarkov, Z.; Stoyanov, L. Application of Supercapacitors in Hybrid Systems. *Proc. Tech. Univ.-Sofia* **2010**, *60*, 299–310.
132. Jagadale, A.; Zhou, X.; Xiong, R.; Dubal, D.P.; Xu, J.; Yang, S. Lithium Ion Capacitors (LICs): Development of the Materials. *Energy Storage Mater.* **2019**, *19*, 314–329. [CrossRef]
133. An, C.; Zhang, Y.; Guo, H.; Wang, Y. Metal Oxide-Based Supercapacitors: Progress and Prospectives. *Nanoscale Adv.* **2019**, *1*, 4644–4658. [CrossRef]
134. Rani, J.; Thangavel, R.; Oh, S.-I.; Lee, Y.; Jang, J.-H. An Ultra-High-Energy Density Supercapacitor; Fabrication Based on Thiol-Functionalized Graphene Oxide Scrolls. *Nanomaterials* **2019**, *9*, 148. [CrossRef]
135. Ge, Y.; Xie, X.; Roscher, J.; Holze, R.; Qu, Q. How to Measure and Report the Capacity of Electrochemical Double Layers, Supercapacitors, and Their Electrode Materials. *J. Solid State Electrochem.* **2020**, *24*, 3215–3230. [CrossRef]
136. Yuan, B.; Liu, J.; Dong, L.; Chen, D.; Zhong, S.; Liang, Y.; Liu, Y.; Ji, Y.; Wu, X.; Kong, Q.; et al. A Single-Layer Composite Separator with 3D-Reinforced Microstructure for Practical High-Temperature Lithium Ion Batteries. *Small* **2022**, *18*, 2107664. [CrossRef] [PubMed]
137. Zhang, S.S. Identifying Rate Limitation and a Guide to Design of Fast-charging Li-ion Battery. *InfoMat* **2020**, *2*, 942–949. [CrossRef]
138. Lu, J.; Wu, T.; Amine, K. State-of-the-Art Characterization Techniques for Advanced Lithium-Ion Batteries. *Nat. Energy* **2017**, *2*, 17011. [CrossRef]
139. Chen, K.; Li, Y.; Zhan, H. Advanced Separators for Lithium-Ion Batteries. *IOP Conf. Ser. Earth Environ. Sci.* **2022**, *1011*, 012009. [CrossRef]
140. Boateng, B.; Zhang, X.; Zhen, C.; Chen, D.; Han, Y.; Feng, C.; Chen, N.; He, W. Recent Advances in Separator Engineering for Effective Dendrite Suppression of Li-metal Anodes. *Nano Sel.* **2021**, *2*, 993–1010. [CrossRef]
141. Zhang, L.; Li, X.; Yang, M.; Chen, W. High-Safety Separators for Lithium-Ion Batteries and Sodium-Ion Batteries: Advances and Perspective. *Energy Storage Mater.* **2021**, *41*, 522–545. [CrossRef]
142. Lizundia, E.; Costa, C.M.; Alves, R.; Lanceros-Méndez, S. Cellulose and Its Derivatives for Lithium Ion Battery Separators: A Review on the Processing Methods and Properties. *Carbohydr. Polym. Technol. Appl.* **2020**, *1*, 100001. [CrossRef]
143. Deimede, V.; Elmasides, C. Separators for Lithium-Ion Batteries: A Review on the Production Processes and Recent Developments. *Energy Technol.* **2015**, *3*, 453–468. [CrossRef]
144. Ren, D.; Feng, X.; Liu, L.; Hsu, H.; Lu, L.; Wang, L.; He, X.; Ouyang, M. Investigating the Relationship between Internal Short Circuit and Thermal Runaway of Lithium-Ion Batteries under Thermal Abuse Condition. *Energy Storage Mater.* **2021**, *34*, 563–573. [CrossRef]
145. Francis, C.F.J.; Kyratzis, I.L.; Best, A.S. Lithium-Ion Battery Separators for Ionic-Liquid Electrolytes: A Review. *Adv. Mater.* **2020**, *32*, 1904205. [CrossRef]
146. Oh, Y.-S.; Jung, G.Y.; Kim, J.-H.; Kim, J.-H.; Kim, S.H.; Kwak, S.K.; Lee, S.-Y. Janus-Faced, Dual-Conductive/Chemically Active Battery Separator Membranes. *Adv. Funct. Mater.* **2016**, *26*, 7074–7083. [CrossRef]
147. Xie, Y.; Zou, H.; Xiang, H.; Xia, R.; Liang, D.; Shi, P.; Dai, S.; Wang, H. Enhancement on the Wettability of Lithium Battery Separator toward Nonaqueous Electrolytes. *J. Memb. Sci.* **2016**, *503*, 25–30. [CrossRef]
148. Nishio, K. PRIMARY BATTERIES–NONAQUEOUS SYSTEMS | Lithium Primary: Overview. In *Encyclopedia of Electrochemical Power Sources*; Elsevier: Amsterdam, The Netherlands, 2009; pp. 68–75.
149. Li, A.; Yuen, A.C.Y.; Wang, W.; De Cachinho Cordeiro, I.M.; Wang, C.; Chen, T.B.Y.; Zhang, J.; Chan, Q.N.; Yeoh, G.H. A Review on Lithium-Ion Battery Separators towards Enhanced Safety Performances and Modelling Approaches. *Molecules* **2021**, *26*, 478. [CrossRef]

150. Lee, H.; Yanilmaz, M.; Toprakci, O.; Fu, K.; Zhang, X. A Review of Recent Developments in Membrane Separators for Rechargeable Lithium-Ion Batteries. *Energy Environ. Sci.* **2014**, *7*, 3857–3886. [CrossRef]
151. Prout, L. Aspects of Lead/Acid Battery Technology 7. Separators. *J. Power Sources* **1993**, *46*, 117–138. [CrossRef]
152. Lv, W.; Zhang, X. Recent Advances in Lithium-Ion Battery Separators with Enhanced Safety. In *60 Years of the Loeb-Sourirajan Membrane*; Elsevier: Amsterdam, The Netherlands, 2022; pp. 269–304.
153. Huang, X. Separator Technologies for Lithium-Ion Batteries. *J. Solid State Electrochem.* **2011**, *15*, 649–662. [CrossRef]
154. Tahalyani, J.; Akhtar, M.J.; Cherusseri, J.; Kar, K.K. Characteristics of Capacitor: Fundamental Aspects. In *Handbook of Nanocomposite Supercapacitor Materials*; Springer: Berlin/Heidelberg, Germany, 2020; pp. 1–51.
155. Liu, Y.; Zhu, Y.; Cui, Y. Challenges and Opportunities towards Fast-Charging Battery Materials. *Nat. Energy* **2019**, *4*, 540–550. [CrossRef]
156. Costa, C.M.; Lee, Y.-H.; Kim, J.-H.; Lee, S.-Y.; Lanceros-Méndez, S. Recent Advances on Separator Membranes for Lithium-Ion Battery Applications: From Porous Membranes to Solid Electrolytes. *Energy Storage Mater.* **2019**, *22*, 346–375. [CrossRef]
157. Zhu, X.; Jiang, X.; Ai, X.; Yang, H.; Cao, Y. A Highly Thermostable Ceramic-Grafted Microporous Polyethylene Separator for Safer Lithium-Ion Batteries. *ACS Appl. Mater. Interfaces* **2015**, *7*, 24119–24126. [CrossRef]
158. Lagadec, M.F.; Zahn, R.; Wood, V. Characterization and Performance Evaluation of Lithium-Ion Battery Separators. *Nat. Energy* **2019**, *4*, 16–25. [CrossRef]
159. Zhang, S.S. A Review on the Separators of Liquid Electrolyte Li-Ion Batteries. *J. Power Sources* **2007**, *164*, 351–364. [CrossRef]
160. Song, J.; Ryou, M.-H.; Son, B.; Lee, J.-N.; Lee, D.J.; Lee, Y.M.; Choi, J.W.; Park, J.-K. Co-Polyimide-Coated Polyethylene Separators for Enhanced Thermal Stability of Lithium Ion Batteries. *Electrochim. Acta* **2012**, *85*, 524–530. [CrossRef]
161. Zhang, X.; Sahraei, E.; Wang, K. Li-Ion Battery Separators, Mechanical Integrity and Failure Mechanisms Leading to Soft and Hard Internal Shorts. *Sci. Rep.* **2016**, *6*, 32578. [CrossRef] [PubMed]
162. Zhang, J.; Yue, L.; Kong, Q.; Liu, Z.; Zhou, X.; Zhang, C.; Xu, Q.; Zhang, B.; Ding, G.; Qin, B.; et al. Sustainable, Heat-Resistant and Flame-Retardant Cellulose-Based Composite Separator for High-Performance Lithium Ion Battery. *Sci. Rep.* **2015**, *4*, 3935. [CrossRef]
163. Xu, Q.; Cheong, Y.-K.; He, S.-Q.; Tiwari, V.; Liu, J.; Wang, Y.; Raja, S.N.; Li, J.; Guan, Y.; Li, W. Suppression of Spinal Connexin 43 Expression Attenuates Mechanical Hypersensitivity in Rats after an L5 Spinal Nerve Injury. *Neurosci. Lett.* **2014**, *566*, 194–199. [CrossRef]
164. Xu, Q.; Kong, Q.; Liu, Z.; Zhang, J.; Wang, X.; Liu, R.; Yue, L.; Cui, G. Polydopamine-Coated Cellulose Microfibrillated Membrane as High Performance Lithium-Ion Battery Separator. *RSC Adv.* **2014**, *4*, 7845. [CrossRef]
165. Liu, A.; Walther, A.; Ikkala, O.; Belova, L.; Berglund, L.A. Clay Nanopaper with Tough Cellulose Nanofiber Matrix for Fire Retardancy and Gas Barrier Functions. *Biomacromolecules* **2011**, *12*, 633–641. [CrossRef]
166. Waqas, M.; Ali, S.; Feng, C.; Chen, D.; Han, J.; He, W. Recent Development in Separators for High-Temperature Lithium-Ion Batteries. *Small* **2019**, *15*, 1901689. [CrossRef]
167. Zhao, Y.; Yue, F.; Li, S.; Zhang, Y.; Tian, Z.; Xu, Q.; Xin, S.; Guo, Y. Advances of Polymer Binders for silicon-based Anodes in High Energy Density lithium-ion Batteries. *InfoMat* **2021**, *3*, 460–501. [CrossRef]
168. Heidari, A.A.; Mahdavi, H.; Karami, M. Recent Advances in Polyolefin-Based Separators for Li-Ion Battery Applications: A Review. *Iran. J. Polym. Sci. Technol.* **2022**, *34*, 423–442. [CrossRef]
169. Li, J.; Dai, L.; Wang, Z.; Wang, H.; Xie, L.; Chen, J.; Yan, C.; Yuan, H.; Wang, H.; Chen, C. Cellulose Nanofiber Separator for Suppressing Shuttle Effect and Li Dendrite Formation in Lithium-Sulfur Batteries. *J. Energy Chem.* **2022**, *67*, 736–744. [CrossRef]
170. Thiangtham, S.; Saito, N.; Manuspiya, H. Asymmetric Porous and Highly Hydrophilic Sulfonated Cellulose/Biomembrane Functioning as a Separator in a Lithium-Ion Battery. *ACS Appl. Energy Mater.* **2022**, *5*, 6206–6218. [CrossRef]
171. Hendricks, C.; Williard, N.; Mathew, S.; Pecht, M. A Failure Modes, Mechanisms, and Effects Analysis (FMMEA) of Lithium-Ion Batteries. *J. Power Sources* **2015**, *297*, 113–120. [CrossRef]
172. McEvoy, A.; Markvart, T.; Castaner, L. *Practical Handbook of Photovoltaics*, 2nd ed.; Elsevier: Amsterdam, The Netherlands, 2012; ISBN 9780123859341.
173. Ruetschi, P. Aging Mechanisms and Service Life of Lead–Acid Batteries. *J. Power Sources* **2004**, *127*, 33–44. [CrossRef]
174. Sun, Y.-H.; Jou, H.-L.; Wu, J.-C. Aging Estimation Method for Lead-Acid Battery. *IEEE Trans. Energy Convers.* **2011**, *26*, 264–271. [CrossRef]
175. Coleman, M.; Hurley, W.G.; Lee, C.K. An Improved Battery Characterization Method Using a Two-Pulse Load Test. *IEEE Trans. Energy Convers.* **2008**, *23*, 708–713. [CrossRef]
176. Gates Energy Products Sealed Lead Cells and Batteries. In *Rechargeable Batteries Applications Handbook*; Elsevier: Amsterdam, The Netherlands, 1998; pp. 153–235; ISBN 9780080515939.
177. Badeda, J.; Huck, M.; Sauer, D.U.; Kabzinski, J.; Wirth, J. Basics of Lead–Acid Battery Modelling and Simulation. In *Lead-Acid Batteries for Future Automobiles*; Elsevier: Amsterdam, The Netherlands, 2017; pp. 463–507.
178. Catherino, H.A.; Feres, F.F.; Trinidad, F. Sulfation in Lead–Acid Batteries. *J. Power Sources* **2004**, *129*, 113–120. [CrossRef]
179. Apăteanu, L.; Hollenkamp, A.F.; Koop, M.J. Electrolyte Stratification in Lead/Acid Batteries: Effect of Grid Antimony and Relationship to Capacity Loss. *J. Power Sources* **1993**, *46*, 239–250. [CrossRef]
180. Pavlov, D. H_2SO_4 Electrolyte—An Active Material in the Lead–Acid Cell. In *Lead-Acid Batteries: Science and Technology*; Elsevier: Amsterdam, The Netherlands, 2017; pp. 133–167.

181. Lin, C.; Tang, A.; Mu, H.; Wang, W.; Wang, C. Aging Mechanisms of Electrode Materials in Lithium-Ion Batteries for Electric Vehicles. *J. Chem.* **2015**, *2015*, 1–11. [CrossRef]
182. Reniers, J.M.; Mulder, G.; Howey, D.A. Review and Performance Comparison of Mechanical-Chemical Degradation Models for Lithium-Ion Batteries. *J. Electrochem. Soc.* **2019**, *166*, A3189–A3200. [CrossRef]
183. Waldmann, T.; Wilka, M.; Kasper, M.; Fleischhammer, M.; Wohlfahrt-Mehrens, M. Temperature Dependent Ageing Mechanisms in Lithium-Ion Batteries–A Post-Mortem Study. *J. Power Sources* **2014**, *262*, 129–135. [CrossRef]
184. Bensebaa, F. Clean Energy. In *Interface Science and Technology*; Elsevier: Amsterdam, The Netherlands, 2013; pp. 279–383.
185. Millange, F.; Férey, G.; Morcrette, M.; Serre, C.; Doublet, M.-L.; Grenèche, J.-M.; Tarascon, J.-M. Towards the Reactivity of MIL-53 or FeIII$(OH)_{0.8}F_{0.2}$[O_2C-C_6H_4-CO_2] versus Lithium. In *Studies in Surface Science and Catalysis*; Elsevier: Amsterdam, The Netherlands, 2007; pp. 2037–2041.
186. Ren, D.; Feng, X.; Lu, L.; He, X.; Ouyang, M. Overcharge Behaviors and Failure Mechanism of Lithium-Ion Batteries under Different Test Conditions. *Appl. Energy* **2019**, *250*, 323–332. [CrossRef]
187. Fedorova, A.A.; Anishchenko, D.V.; Beletskii, E.V.; Kalnin, A.Y.; Levin, O.V. Modeling of the Overcharge Behavior of Lithium-Ion Battery Cells Protected by a Voltage-Switchable Resistive Polymer Layer. *J. Power Sources* **2021**, *510*, 230392. [CrossRef]
188. Birkl, C.R.; Roberts, M.R.; McTurk, E.; Bruce, P.G.; Howey, D.A. Degradation Diagnostics for Lithium Ion Cells. *J. Power Sources* **2017**, *341*, 373–386. [CrossRef]
189. Sreenarayanan, B.; Tan, D.H.S.; Bai, S.; Li, W.; Bao, W.; Meng, Y.S. Quantification of Lithium Inventory Loss in Micro Silicon Anode via Titration-Gas Chromatography. *J. Power Sources* **2022**, *531*, 231327. [CrossRef]
190. Edge, J.S.; O'Kane, S.; Prosser, R.; Kirkaldy, N.D.; Patel, A.N.; Hales, A.; Ghosh, A.; Ai, W.; Chen, J.; Yang, J.; et al. Lithium Ion Battery Degradation: What You Need to Know. *Phys. Chem. Chem. Phys.* **2021**, *23*, 8200–8221. [CrossRef]
191. Pender, J.P.; Jha, G.; Youn, D.H.; Ziegler, J.M.; Andoni, I.; Choi, E.J.; Heller, A.; Dunn, B.S.; Weiss, P.S.; Penner, R.M.; et al. Electrode Degradation in Lithium-Ion Batteries. *ACS Nano* **2020**, *14*, 1243–1295. [CrossRef]
192. Lin, X.; Khosravinia, K.; Hu, X.; Li, J.; Lu, W. Lithium Plating Mechanism, Detection, and Mitigation in Lithium-Ion Batteries. *Prog. Energy Combust. Sci.* **2021**, *87*, 100953. [CrossRef]
193. Kreczanik, P.; Venet, P.; Hijazi, A.; Clerc, G. Study of Supercapacitor Aging and Lifetime Estimation According to Voltage, Temperature, and RMS Current. *IEEE Trans. Ind. Electron.* **2014**, *61*, 4895–4902. [CrossRef]
194. Murray, D.B.; Hayes, J.G. Cycle Testing of Supercapacitors for Long-Life Robust Applications. *IEEE Trans. Power Electron.* **2015**, *30*, 2505–2516. [CrossRef]
195. Rizoug, N.; Bartholomeus, P.; Le Moigne, P. Study of the Ageing Process of a Supercapacitor Module Using Direct Method of Characterization. *IEEE Trans. Energy Convers.* **2012**, *27*, 220–228. [CrossRef]
196. Bohlen, O.; Kowal, J.; Sauer, D.U. Ageing Behaviour of Electrochemical Double Layer Capacitors. *J. Power Sources* **2007**, *172*, 468–475. [CrossRef]
197. Gualous, H.; Louahlia, H.; Gallay, R. Supercapacitor Characterization and Thermal Modelling With Reversible and Irreversible Heat Effect. *IEEE Trans. Power Electron.* **2011**, *26*, 3402–3409. [CrossRef]
198. German, R.; Sari, A.; Briat, O.; Vinassa, J.-M.; Venet, P. Impact of Voltage Resets on Supercapacitors Aging. *IEEE Trans. Ind. Electron.* **2016**, *63*, 7703–7711. [CrossRef]
199. German, R.; Sari, A.; Venet, P.; Ayadi, M.; Briat, O.; Vinassa, J.M. Prediction of Supercapacitors Floating Ageing with Surface Electrode Interface Based Ageing Law. *Microelectron. Reliab.* **2014**, *54*, 1813–1817. [CrossRef]
200. Azaïs, P.; Duclaux, L.; Florian, P.; Massiot, D.; Lillo-Rodenas, M.-A.; Linares-Solano, A.; Peres, J.-P.; Jehoulet, C.; Béguin, F. Causes of Supercapacitors Ageing in Organic Electrolyte. *J. Power Sources* **2007**, *171*, 1046–1053. [CrossRef]
201. Liu, Y.; Huang, Z.; Liao, H.; Lyu, C.; Zhou, Y.; Jiao, Y.; Li, H.; Hu, C.; Peng, J. A Temperature-Suppression Charging Strategy for Supercapacitor Stack With Lifetime Maximization. *IEEE Trans. Ind. Appl.* **2019**, *55*, 6173–6183. [CrossRef]
202. Karimi-Maleh, H.; Karimi, F.; Alizadeh, M.; Sanati, A.L. Electrochemical Sensors, a Bright Future in the Fabrication of Portable Kits in Analytical Systems. *Chem. Rec.* **2020**, *20*, 682–692. [CrossRef]
203. Karimi-Maleh, H.; Ayati, A.; Ghanbari, S.; Orooji, Y.; Tanhaei, B.; Karimi, F.; Alizadeh, M.; Rouhi, J.; Fu, L.; Sillanpää, M. Recent Advances in Removal Techniques of Cr(VI) Toxic Ion from Aqueous Solution: A Comprehensive Review. *J. Mol. Liq.* **2021**, *329*, 115062. [CrossRef]
204. Fu, L.; Xie, K.; Wu, D.; Wang, A.; Zhang, H.; Ji, Z. Electrochemical Determination of Vanillin in Food Samples by Using Pyrolyzed Graphitic Carbon Nitride. *Mater. Chem. Phys.* **2020**, *242*, 122462. [CrossRef]
205. Fu, L.; Wang, Q.; Zhang, M.; Zheng, Y.; Wu, M.; Lan, Z.; Pu, J.; Zhang, H.; Chen, F.; Su, W.; et al. Electrochemical Sex Determination of Dioecious Plants Using Polydopamine-Functionalized Graphene Sheets. *Front. Chem.* **2020**, *8*, 92. [CrossRef] [PubMed]
206. Yuan, Z.; Xue, N.; Xie, J.; Xu, R.; Lei, C. Separator Aging and Performance Degradation Caused by Battery Expansion: Cyclic Compression Test Simulation of Polypropylene Separator. *J. Electrochem. Soc.* **2021**, *168*, 030506. [CrossRef]
207. Zhang, X.; Zhu, J.; Sahraei, E. Degradation of Battery Separators under Charge–Discharge Cycles. *RSC Adv.* **2017**, *7*, 56099–56107. [CrossRef]
208. Chen, J.; Yan, Y.; Sun, T.; Qi, Y.; Li, X. Probing the Roles of Polymeric Separators in Lithium-Ion Battery Capacity Fade at Elevated Temperatures. *J. Electrochem. Soc.* **2014**, *161*, A1241–A1246. [CrossRef]
209. Yan, S.; Xiao, X.; Huang, X.; Li, X.; Qi, Y. Unveiling the Environment-Dependent Mechanical Properties of Porous Polypropylene Separators. *Polymer* **2014**, *55*, 6282–6292. [CrossRef]

210. Lithium-Secondary Cell. In *Electrochemical Power Sources: Fundamentals, Systems, and Applications*; Elsevier: Amsterdam, The Netherlands, 2019; pp. 143–266.
211. Rahimi-Eichi, H.; Ojha, U.; Baronti, F.; Chow, M.-Y. Battery Management System: An Overview of Its Application in the Smart Grid and Electric Vehicles. *IEEE Ind. Electron. Mag.* **2013**, *7*, 4–16. [CrossRef]
212. Faisal, M.; Hannan, M.A.; Ker, P.J.; Hossain Lipu, M.S.; Uddin, M.N. Fuzzy-Based Charging–Discharging Controller for Lithium-Ion Battery in Microgrid Applications. *IEEE Trans. Ind. Appl.* **2021**, *57*, 4187–4195. [CrossRef]
213. Verbrugge, M.W. Adaptive Characterization and Modeling of Electrochemical Energy Storage Devices for Hybrid Electric Vehicle Applications. In *Modeling and Numerical Simulations*; Springer: Berlin/Heidelberg, Germany, 2008; pp. 417–524.
214. Verbrugge, M.; Koch, B. Generalized Recursive Algorithm for Adaptive Multiparameter Regression. *J. Electrochem. Soc.* **2006**, *153*, A187. [CrossRef]
215. Verbrugge, M.W.; Conell, R.S. Electrochemical and Thermal Characterization of Battery Modules Commensurate with Electric Vehicle Integration. *J. Electrochem. Soc.* **2002**, *149*, A45. [CrossRef]
216. Wang, B.; Xu, J.; Cao, B.; Ning, B. Adaptive Mode Switch Strategy Based on Simulated Annealing Optimization of a Multi-Mode Hybrid Energy Storage System for Electric Vehicles. *Appl. Energy* **2017**, *194*, 596–608. [CrossRef]
217. Guo, M.; Sikha, G.; White, R.E. Single-Particle Model for a Lithium-Ion Cell: Thermal Behavior. *J. Electrochem. Soc.* **2011**, *158*, A122. [CrossRef]
218. Arora, S.; Abkenar, A.T.; Jayasinghe, S.G.; Tammi, K. Battery Management System: Charge Balancing and Temperature Control. In *Heavy-Duty Electric Vehicles*; Elsevier: Amsterdam, The Netherlands, 2021; pp. 173–203.
219. Wang, P.; Zhu, C. Summary of Lead-Acid Battery Management System. *IOP Conf. Ser. Earth Environ. Sci.* **2020**, *440*, 022014. [CrossRef]
220. Vezzini, A. Lithium-Ion Battery Management. In *Lithium-Ion Batteries*; Elsevier: Amsterdam, The Netherlands, 2014; pp. 345–360.
221. Qazi, S. Portable Standalone PV Systems for Disaster Relief and Remote Areas. In *Standalone Photovoltaic (PV) Systems for Disaster Relief and Remote Areas*; Elsevier: Amsterdam, The Netherlands, 2017; pp. 113–138.
222. Murtaza, A.F.; Chiaberge, M.; Spertino, F.; Ahmad, J.; Ciocia, A. A Direct PWM Voltage Controller of MPPT & Sizing of DC Loads for Photovoltaic System. *IEEE Trans. Energy Convers.* **2018**, *33*, 991–1001. [CrossRef]
223. Antonov, I.; Kanchev, H.; Hinov, N. Study of PWM Solar Charge Controller Operation Modes in Autonomous DC System. In Proceedings of the 2019 II International Conference on High Technology for Sustainable Development (HiTech), Sofia, Bulgaria, 10–11 October 2019; IEEE: New York, NY, USA, 2019; pp. 1–4.
224. Acharya, P.S.; Aithal, P.S. A Comparative Study of MPPT and PWM Solar Charge Controllers and Their Integrated System. *J. Phys. Conf. Ser.* **2020**, *1712*, 012023. [CrossRef]
225. Rezoug, M.R.; Chenni, R.; Taibi, D. A New Approach for Optimizing Management of a Real Time Solar Charger Using the Firebase Platform Under Android. *J. Low Power Electron. Appl.* **2019**, *9*, 23. [CrossRef]
226. Bhattacharjee, A.; Samanta, H.; Banerjee, N.; Saha, H. Development and Validation of a Real Time Flow Control Integrated MPPT Charger for Solar PV Applications of Vanadium Redox Flow Battery. *Energy Convers. Manag.* **2018**, *171*, 1449–1462. [CrossRef]
227. Monden, Y.; Mizutani, M.; Yamazaki, S.; Kobayashi, T. Charging and Discharging Control of a Hybrid Battery Energy Storage System Using Different Battery Types in Order to Avoid Degradation. In Proceedings of the 2021 IEEE International Future Energy Electronics Conference (IFEEC), Taipei, Taiwan, 16 November 2021; IEEE: New York, NY, USA, 2021; pp. 1–6.
228. Garcia, P.; Fernandez, L.M.; Garcia, C.A.; Jurado, F. Energy Management System of Fuel-Cell-Battery Hybrid Tramway. *IEEE Trans. Ind. Electron.* **2010**, *57*, 4013–4023. [CrossRef]
229. Shen, J.; Khaligh, A. A Supervisory Energy Management Control Strategy in a Battery/Ultracapacitor Hybrid Energy Storage System. *IEEE Trans. Transp. Electrif.* **2015**, *1*, 223–231. [CrossRef]
230. Carter, R.; Cruden, A.; Hall, P.J. Optimizing for Efficiency or Battery Life in a Battery/Supercapacitor Electric Vehicle. *IEEE Trans. Veh. Technol.* **2012**, *61*, 1526–1533. [CrossRef]
231. Santucci, A.; Sorniotti, A.; Lekakou, C. Power Split Strategies for Hybrid Energy Storage Systems for Vehicular Applications. *J. Power Sources* **2014**, *258*, 395–407. [CrossRef]
232. Townsend, A.; Martinson, C.; Gouws, R.; Bessarabov, D. Effect of Supercapacitors on the Operation of an Air-Cooled Hydrogen Fuel Cell. *Heliyon* **2021**, *7*, e06569. [CrossRef] [PubMed]
233. Chen, H.; Xiong, R.; Member, S.; Lin, C.; Shen, W. Model Predictive Control Based Real-Time Energy Management for a Hybrid Energy Storage System. *CSEE J. Power Energy Syst.* **2020**, *7*, 862–874. [CrossRef]
234. Hannan, M.A.; Hoque, M.M.; Mohamed, A.; Ayob, A. Review of Energy Storage Systems for Electric Vehicle Applications: Issues and Challenges. *Renew. Sustain. Energy Rev.* **2017**, *69*, 771–789. [CrossRef]
235. Ren, G.; Ma, G.; Cong, N. Review of Electrical Energy Storage System for Vehicular Applications. *Renew. Sustain. Energy Rev.* **2015**, *41*, 225–236. [CrossRef]
236. Song, Z.; Hofmann, H.; Li, J.; Han, X.; Ouyang, M. Optimization for a Hybrid Energy Storage System in Electric Vehicles Using Dynamic Programing Approach. *Appl. Energy* **2015**, *139*, 151–162. [CrossRef]
237. Ramoul, J.; Chemali, E.; Dorn-Gomba, L.; Emadi, A. A Neural Network Energy Management Controller Applied to a Hybrid Energy Storage System Using Multi-Source Inverter. In Proceedings of the 2018 IEEE Energy Conversion Congress and Exposition (ECCE), Portland, OR, USA, 23–27 September 2018; IEEE: New York, NY, USA, 2018; pp. 2741–2747.

238. Xiong, R.; Cao, J.; Yu, Q. Reinforcement Learning-Based Real-Time Power Management for Hybrid Energy Storage System in the Plug-in Hybrid Electric Vehicle. *Appl. Energy* **2018**, *211*, 538–548. [CrossRef]
239. Salmasi, F.R. Control Strategies for Hybrid Electric Vehicles: Evolution, Classification, Comparison, and Future Trends. *IEEE Trans. Veh. Technol.* **2007**, *56*, 2393–2404. [CrossRef]
240. Xiong, R.; Chen, H.; Wang, C.; Sun, F. Towards a Smarter Hybrid Energy Storage System Based on Battery and Ultracapacitor—A Critical Review on Topology and Energy Management. *J. Clean. Prod.* **2018**, *202*, 1228–1240. [CrossRef]
241. Trovão, J.P.; Pereirinha, P.G.; Jorge, H.M.; Antunes, C.H. A Multi-Level Energy Management System for Multi-Source Electric Vehicles–An Integrated Rule-Based Meta-Heuristic Approach. *Appl. Energy* **2013**, *105*, 304–318. [CrossRef]
242. Schouten, N.J.; Salman, M.A.; Kheir, N.A. Energy Management Strategies for Parallel Hybrid Vehicles Using Fuzzy Logic. *Control Eng. Pract.* **2003**, *11*, 171–177. [CrossRef]
243. Zandi, M.; Payman, A.; Martin, J.-P.; Pierfederici, S.; Davat, B.; Meibody-Tabar, F. Energy Management of a Fuel Cell/Supercapacitor/Battery Power Source for Electric Vehicular Applications. *IEEE Trans. Veh. Technol.* **2011**, *60*, 433–443. [CrossRef]
244. Hung, Y.-H.; Wu, C.-H. An Integrated Optimization Approach for a Hybrid Energy System in Electric Vehicles. *Appl. Energy* **2012**, *98*, 479–490. [CrossRef]
245. Song, Z.; Hofmann, H.; Li, J.; Hou, J.; Han, X.; Ouyang, M. Energy Management Strategies Comparison for Electric Vehicles with Hybrid Energy Storage System. *Appl. Energy* **2014**, *134*, 321–331. [CrossRef]
246. Hredzak, B.; Agelidis, V.G.; Jang, M. A Model Predictive Control System for a Hybrid Battery-Ultracapacitor Power Source. *IEEE Trans. Power Electron.* **2014**, *29*, 1469–1479. [CrossRef]
247. Zhang, S.; Xiong, R.; Sun, F. Model Predictive Control for Power Management in a Plug-in Hybrid Electric Vehicle with a Hybrid Energy Storage System. *Appl. Energy* **2017**, *185*, 1654–1662. [CrossRef]
248. Sun, C.; Hu, X.; Moura, S.J.; Sun, F. Velocity Predictors for Predictive Energy Management in Hybrid Electric Vehicles. *IEEE Trans. Control Syst. Technol.* **2015**, *23*, 1197–1204. [CrossRef]
249. Song, K.S.; Park, S.-J.; Kang, F.-S. Internal Parameter Estimation of Lithium-Ion Battery Using AC Ripple With DC Offset Wave in Low and High Frequencies. *IEEE Access* **2021**, *9*, 76083–76096. [CrossRef]
250. Moral, C.G.; Laborda, D.F.; Alonso, L.S.; Guerrero, J.M.; Fernandez, D.; Rivas Pereda, C.; Reigosa, D.D. Battery Internal Resistance Estimation Using a Battery Balancing System Based on Switched Capacitors. *IEEE Trans. Ind. Appl.* **2020**, *56*, 5363–5374. [CrossRef]